AN ABSTRACT OF THE THESIS OF

Sarah G. Nalven for the degree of Master of Science in Ocean, Earth, and Atmospheric Sciences presented on July 7, 2016.

Title: Decoding DOM Degradation with Metatranscriptomics: How Do Sunlight and Microbial Communities Interact to Degrade Dissolved Organic Matter in Arctic Freshwaters?

Abstract approved:

Byron C. Crump

Arctic soils are warming, making vast stores of organic carbon available for conversion to CO_2. This could create a positive feedback loop and accelerate global warming, but the processes that convert this carbon into CO_2 are not well understood. We investigated how the combined activities of sunlight and microbes degrade soil dissolved organic matter (DOM), an important component of the carbon processed in arctic freshwaters. DOM leached from the organic layer of moist acidic tundra was exposed to natural sunlight (24 h) or kept in the dark, inoculated and incubated with a soil microbial community, and analyzed for DOM composition (FT-ICR MS) and microbial gene expression (metatranscriptomics). We found that DOM degraded by sunlight was similar in composition to DOM degraded by microbes, and consequently, microbial

activity was lower when incubated with sunlight-exposed DOM. We also found sunlight-exposed DOM caused global shifts in both microbial gene expression and the taxonomic groups conducting this expression. Greater expression of transcription and translation genes suggested growth, while lower expression of metabolism, motility, and transport genes suggested reduced investment in scavenging. Photo-exposure of DOM also caused reduced expression of enzymes involved in aromatic degradation, oxygenases, and decarboxylases, suggesting sunlight degraded aromatics, oxidized DOM, and decarboxylated DOM. Shifts in expression of transporters for small, labile compounds and nutrient-containing compounds suggested photo-exposure may have altered bioavailability of these compounds in the DOM pool. These findings demonstrate that even small amounts of sunlight can alter DOM in ways that evoke profound changes in microbial functioning, supporting the idea that sunlight plays a key role in determining the microbial processing of DOM in arctic freshwaters.

Decoding DOM Degradation with Metatranscriptomics: How Do Sunlight and Microbial Communities Interact to Degrade Dissolved Organic Matter in Arctic Freshwaters?

by
Sarah G. Nalven

A THESIS

submitted to

Oregon State University

in partial fulfillment of
the requirements for the
degree of

Master of Science

Presented July 7, 2016
Commencement June 2017

Master of Science thesis of Sarah G. Nalven presented on July 7, 2016

APPROVED:

Major Professor, representing Ocean, Earth, and Atmospheric Sciences

Dean of the College of Earth, Ocean, and Atmospheric Sciences

Dean of the Graduate School

I understand that my thesis will become part of the permanent collection of Oregon State University libraries. My signature below authorizes release of my thesis to any reader upon request.

Sarah G. Nalven, Author

ACKNOWLEDGEMENTS

I could not have completed this project alone. First, I'd like to thank my advisor, Byron Crump, who was exceptionally generous with his time and energy. We spent some long hours in his office, struggling with code and puzzling over data, and I am so grateful that he was always ready to team up if I asked. I'm also thankful for his high expectations and continuous patience.

I am indebted to my collaborators, Drs. Collin Ward, Rose Cory, and George Kling, who designed and carried out the field component of this study and provided critical assistance throughout this process. Thanks especially to Collin, who conducted the chemical analyses for this project, and who succumbed to barrages of emails and phone calls over the last year.

My committee members, Drs. Thomas Sharpton, Andrew Thurber, and David Myrold, were also instrumental in moving my project along. Tom is an inspirational bioinformatician. Working with him in the early stages of my analysis, as I barely knew how to write one line of code, really jump-started my project and bioinformatic abilities, and I always appreciated his time and patience. I could always count on Andrew to help me make a difficult decision—whether it regarded courses, figures, statistics or more, he was always equipped to reason things through and end a meeting with an answer.

I am grateful for the advice of several other OSU professors, including Drs. Rick Colwell, Ricardo Letelier, Ryan Mueller, Yuan Jiang and Yanming Di. Our Geomicro seminar group at OSU also always provided a comfortable

environment to share ideas, pose questions, and practice talks. Past and current members of the Crump, Cory, and Kling labs (and other Toolik friends) also deserve many thanks for assistance in the field and lab, and just good ol' camaraderie. Days at a remote field station can be long, but it was the jokes, stories, and shared love of the natural world that made it all worth it. A special thanks to Jason Dobkowski— our research group is very lucky to have you around, and to Jerome Payet—I'm very glad you joined our lab.

Of course, many thanks to my friends and family, near and far, who supported me through a challenging two years, and many of whom were also willing to talk through thesis-related roadblocks. In Corvallis, Mike Graw, Stacey Detwiler, and Erin Peck probably heard more about dissolved organic matter, microbes and RNA extractions than they could have ever imagined (or wanted). Back east, Dan Ackerman and my parents also got their fill of shop talk, and helped keep me sane and happy.

Finally, this project could not have been completed without support from the management and staff of several organizations, including Toolik Field Station, the Joint Genome Institute (namely Tijana Glavina del Rio), and OSU's Center for Genome Research and Biocomputing (namely Chris Sullivan). I am also grateful for grants from the National Science Foundation's LTREB program (DEB-1147378/1347042), and the Department of Energy's JGI-EMSL Collaborative Science Initiative (CSP 1782).

TABLE OF CONTENTS

Page

1. Introduction..……1

2. Methods…….……..5

2.1. Sample collection……5

2.2. Experimental design……...5

2.3. Laboratory analysis……6

2.3.1. Characterization of DOM……....6

2.3.2. Characterization of microbial activity……7

2.3.3. RNA extraction and sequencing……7

2.3.4. DNA extraction and 16S amplicon sequencing……..8

2.4. Bioinformatic & statistical analysis……...9

2.4.1. Characterization of DOM……9

2.4.2. Characterization of microbial activity……..10

2.4.3. Metatranscriptomics of microbial communities……10

2.4.4. Microbial community composition……...13

3. Results…….....14

3.1. Effect of photochemical and biological degradation of DOM.....14

3.2. Global response of microbial communities to DOM source……...16

3.3. Genetic evidence for sunlight's effect on DOM……19

3.4. Taxonomic response to DOM source……23

4. Discussion…….....26

4.1. Effect of photochemical and biological degradation of DOM…….26

TABLE OF CONTENTS (Continued)

Page

4.2. Global response of microbial communities to DOM source……...29

4.3. Genetic evidence for sunlight's effect on DOM……37

4.4. Taxonomic response to DOM source……44

5. Conclusion……49

6. Bibliography……....51

7. Figures …..……..……62

LIST OF FIGURES

Figure Page

Figure 1. Schematic of experimental design……63

Figure 2. Effect of photochemical and biological degradation on DOM……..64

Figure 3. Microbial activity across treatments……..65

Figure 4. Characterization of gene expression across treatments……...66

Figure 5. Expression of KEGG tier II and III categories across treatments…67

Figure 6. Genetic evidence for sunlight's effect on DOM……..68

Figure 7. Taxonomic composition of whole and active communities……...69

1. INTRODUCTION

Terrestrially derived dissolved organic matter (DOM) is an important component of the carbon processed in arctic freshwaters (Kling et al., 1991). This component has the potential to grow as the Arctic warms and vast stores of soil carbon are thawed and released to surface waters (Rowland et al., 2010). If converted to greenhouse gases, this carbon could create a positive feedback loop and accelerate global warming (Schuur et al., 2009). However, the fate of this carbon is unknown, in large part because the factors controlling DOM degradation are poorly understood.

Once soil carbon enters surface water as DOM, it is transformed and mineralized by the combined activities of microbes and sunlight (Cole et al., 2007; Cory et al., 2014); but little is known about the biological and photochemical reactions that degrade DOM in surface waters, or how these reactions interact. In fact, numerous studies have found that exposing DOM to sunlight can either increase or decrease DOM's lability to bacteria, but to our knowledge, no study has revealed the mechanisms behind these contrasting effects (e.g., Cory et al., 2013; Obernosterer et al., 1999; Tranvik & Bertilsson, 2001; Vallieres et al., 2008). Evidence suggests that DOM source and history, and microbial community composition, together determine how sunlight exposure affects DOM and how microbial activity will respond to these effects (Cory et al., 2013; Cory et al., 2014; Crump et al., 2003; Judd et al., 2007; Logue et al., 2015; Obernosterer et al., 1999; Tranvik & Bertilsson, 2001). However, a mechanistic understanding of DOM degradation is lacking,

despite its critical importance to modeling the global carbon cycle and accurately predicting climate change.

To address this lack in understanding, it is necessary to determine 1) how sunlight alters the diverse set of compounds in the DOM pool and 2) how microbial communities use DOM differently once it has been exposed to sunlight. Regarding the former, it is widely recognized that photo-degradation mineralizes DOM to CO_2 and CO, transforms DOM to new, smaller compounds, and alters concentrations of dissolved nutrients such as nitrogen, phosphorus and iron (Mopper et al., 2014; Moran & Zepp, 1997). Still we cannot predict if and how sunlight will affect different fractions of the DOM pool. Regarding the latter, although we have identified many of the proteins and metabolic pathways that allow microbial communities to access and degrade DOM, we do not have a firm grasp on how the composition of DOM relates to its biolability. For example, although the prevailing paradigm of biolability considers low molecular weight compounds to be preferable to microorganisms (Hopkinson et al., 1998), mounting evidence suggests that high molecular weight compounds can be labile as well (Cory & Kaplan, 2012; Frazier et al., 2005; Mann et al., 2012; Wetzel, 2003; Sleighter et al., 2014; Volk et al., 1997; Ward et al., 2013). Thus, in order to predict the fate of DOM in surface waters, it is important to clarify the molecular level controls on both photochemical and biological DOM degradation.

Obtaining a molecular-level understanding of DOM degradation is difficult in part because standard analytical techniques cannot identify the

thousands of compounds that make up DOM pools. Several methods offer bulk assessments of DOM, Mass Spectrometry identifies the molecular formulas present, and Nuclear Magnetic Resonance recognizes functional components within compounds. However, no technology exists to identify the suite of individual compounds (i.e., formula and structural arrangement) composing DOM mixtures. Currently, the most accurate and resolved analysis of DOM chemical composition is obtained with Fourier transform ion cyclotron resonance mass spectrometry (FT-ICR MS). This ultra-high resolution technique allows detection of thousands of individual formulas that make up the DOM pool. It does not, however, provide any information on the structural arrangement of formulas and thus does not provide the identity of the compounds themselves.

Therefore we paired FT-ICR MS with a genomic approach, specifically metatranscriptomics, a technique that identifies expressed genes of microbial communities through analysis of a sample's mRNA sequences. Metatranscriptomics can be used to infer active metabolic processes within microbial communities and the taxa carrying out these processes (Frias-Lopez et al., 2011). It can also provide information about carbon turnover and the DOM compounds associated with this turnover (McCarren et al., 2010; Poretsky et al., 2010). Thus metatranscriptomics, like FT-ICR MS, can provide sensitive detection of changes to DOM, but unlike FT-ICR MS, can allow identification of compounds rather than just their chemical formulas. Metatranscriptomics also detects DOM changes only if they are relevant to

microbial communities, complimenting FT-ICR MS, which detects all types of DOM changes. However, studies have rarely linked community expression patterns to the chemical composition of DOM, leaving the relationship between DOM composition and microbial metabolism poorly understood. Here, we paired FT-ICR MS with metatranscriptomics to gain molecular insight into this relationship that could not have been achieved with other methods. We used both FT-ICR MS and metatranscriptomics to detect sunlight-induced changes to DOM, and used metatranscriptomics to explain microbial responses to photo-exposed DOM.

To investigate the photochemical and biological mechanisms of DOM degradation, we conducted an experiment comparing the character and microbial metabolism of DOM that was exposed to natural sunlight to DOM that was kept in the dark. We characterized DOM before and after sunlight exposure, and after subsequent microbial degradation using FT-ICR MS. Then we characterized microbial metabolism of light-exposed and dark-control DOM using metatranscriptomics. By comparing DOM and its metabolism in this way, we captured a more mechanistic understanding of DOM degradation, one that is critical to estimating arctic carbon budgets and forecasting global climate change.

2. METHODS

2.1. Sample collection

Site and sample collection were previously described in detail (Ward & Cory, 2015). Soil samples from three adjacent pits were collected at 5-15 cm depth on June 15, 2013 in the Imnavait Creek watershed on the North Slope of Alaska (68.62° N, 149.28° W; elevation ~ 900 m). Soil was collected in ziplock bags, immediately transferred to coolers, and within hours, placed in freezers at Toolik Field Station.

2.2. Experimental design

Microbial communities were incubated in triplicate with both light-exposed and dark-control soil-derived DOM (Fig. 1). Soil from each pit (3600 g) was thawed and leached overnight in 14 L of sterile water. Leaching took place inside acid- and DI-rinsed HDPE buckets at room temperature. The dissolved fraction of the soil leachate, from here on referred to as DOM, was isolated with 50, 20 and 10 μm nylon screens (Cole-Parmer, Inc.) and 5 and 0.45 μm high-capacity cartridge filters (Geotech Environmental Equipment, Inc.). Light exposure of DOM took place at Toolik Field Station on June 24 and 25, 2013, where light-exposed replicates (5L) were placed in UV-transparent Whirlpak bags and exposed to about 24 h of natural sunlight. Dark-control replicates (5L) were placed next to light-exposed replicates, but in foil-wrapped Whirlpak bags. After light exposure, subsamples of DOM were collected for characterization with FT-ICR MS and other analytical methods.

DOM was then inoculated with a mixture of all three GF/C (Whatman) filtered leachates (equivalent to 20% of the leachate volume) and incubated in the dark at 6-7 °C. After 4 h, subsamples were filtered and preserved for DNA and RNA analysis. After 5 d, subsamples were collected for DOM characterization with FT-ICR MS. Subsamples were also incubated separately over 5 d for respiration measurements (O_2 consumption and CO_2 production), taken at 0 and 5 d time-points for cell counts, and taken at 5 d for bacterial production.

2.3. Laboratory analysis

2.3.1. Characterization of DOM

High-resolution mass spectra were acquired using a 12 T Bruker SolariX FT-ICR mass spectrometer. Sample preparation (whole water extraction), acquisition parameters, and formula assignment criteria were previously described in detail (Ward & Cory, 2015). To compensate for some of the limitations of FT-ICR MS, Orbitrap mass spectrometry (MS) was used to detect low-mass formulas (detailed in Ward & Cory, 2016) and ^{13}C NMR to assess functional group distribution (detailed in Ward & Cory, 2015). Bulk characterization of DOM, including quantification of chromophoric and fluorescent DOM fractions, used UV−visible absorbance and fluorescence spectroscopy with a Horiba Scientific Aqualog (detailed in Ward & Cory, 2015). Dissolved organic carbon concentration was quantified as CO_2 after high-temperature catalytic combustion using potassium hydrogen phthalate as the calibration standard (Shimadzu Corporation; Kling et al., 2000).

2.3.2. Characterization of microbial activity

Bacterial concentrations, respiration, production, and growth efficiency were quantified as described in Ward & Cory (2015). Briefly, bacterial concentrations were quantified using epifluorescence microscopy to visualize glutaraldehyde-fixed samples (Crump et al., 1998). Respiration was measured as CO_2 production and O_2 consumption relative to killed controls (1% $HgCl_2$). Membrane inlet mass spectrometry was used to measure O_2, and a DIC analyzer (Apollo Sci Tech, LLC) was used to measure CO_2. Bacterial production was determined by measuring ^{14}C-labeled L-leucine incorporation into cells in two subsamples and one TCA-killed control incubated for 2-4 h at 6 °C in the dark.

2.3.3. RNA extraction and sequencing

RNA samples were filtered onto 0.22-µm polyethersulfone (Supor) membrane filters (Pall Corp.) and preserved with RNA*later*™ RNA Stabilization Reagent (Qiagen). RNA extraction and DNA removal was carried out as described by Poretsky et al. (2009). This protocol modifies the RNeasy mini kit protocol (Qiagen) and uses the TURBO DNA-free kit (Ambion).

Ribosomal RNA removal, cDNA synthesis and Illumina HiSeq sequencing were performed at the Joint Genome Institute in Walnut Creek, CA. They used either their standard or low-input RNASeq protocol, depending on the amount of sample available. In both protocols, rRNA was removed from 1 µg or 100 ng of total RNA (regular vs. low-input protocol, respectively)

using the Ribo-Zero™ rRNA Removal Kit for Bacteria (Epicentre). Stranded cDNA libraries were generated using the Illumina Truseq Stranded RNA LT kit. The rRNA depleted-RNA was fragmented and reverse transcribed using random hexamers and SSII (Invitrogen) followed by second strand synthesis. The fragmented cDNA was treated with end-pair, A-tailing, adapter ligation, and 8 or 10 cycles of PCR (regular vs. low-input protocol, respectively). The quantified libraries were then multiplexed into pools of 4 or 3 libraries (regular vs. low-input protocol, respectively), and the pool was then prepared for sequencing on the Illumina HiSeq sequencing platform using a TruSeq paired-end cluster kit, v4, and Illumina's cBot instrument to generate a clustered flowcell for sequencing. Sequencing of the flowcell was performed on the Illumina HiSeq2500 sequencer using HiSeq TruSeq SBS sequencing kits, v4, following a 2x150 indexed run recipe.

2.3.4. DNA extraction and 16S amplicon sequencing

Bacterial community composition was determined with amplification and sequencing of the 16S ribosomal RNA gene. DNA samples were collected, preserved and extracted as previously described (Crump et al., 2003) using methods adapted from Zhou et al. (1996). PCR amplicon sequencing of extracted DNA followed the Earth Microbiome Project protocol (http://www.earthmicrobiome.org/emp-standard-protocols/16s/): Primers focused on the V4 region of the 16S rRNA gene (515F, GTGCCAGCMGCCGCGGTAA and 806R, GGACTACHVGGGTWTCTAAT), and were combined at 250 nM with template DNA, sterile water and

HotMasterMix (5Prime) under the following conditions: 94°C for 3 min; 30 cycles of 94°C for 45 sec, 50°C for 60 sec, 72°C for 90 sec; 72°C for 10 min. Triplicate amplifications were pooled, quantified with Picogreen, combined in equimolar concentrations, and cleaned using the Ultraclean PCR Clean-Up Kit (MoBio). Finally, samples were sequenced at Oregon State University's Center for Genome Research and Biocomputing with Illumina MiSeq 2x150 bp paired-end reads.

2.4. Bioinformatic and statistical analysis

2.4.1. Characterization of DOM

FT-ICR mass spectra were analyzed according to Ward & Cory (2015). Formulas were classified as aromatic, aliphatic, and highly-oxidized tannin-like compounds on the basis of their chemical composition as in Ward & Cory (2016). Formulas were also tested for significant differences in peak intensity with Spearman correlations according to Ward & Cory (2016). The percent of DOM that was mineralized to CO_2 was determined by dividing the amount of CO_2 produced by the initial amount of dissolved organic carbon. The percent of DOM consumed or altered by sunlight was determined by adding mineralized DOM and partially oxidized DOM (Ward & Cory, 2016). Changes to the chromophoric and fluorescent fraction of DOM were quantified using absorption coefficients following Ward & Cory (2016). Changes in molecular weight of DOM were quantified using the slope ratio following Helms et al. (2008). ^{13}C NMR followed protocols described in Ward & Cory (2016).

Orbitrap MS followed Remucal et al. (2012) as described in Ward & Cory (2016).

2.4.2. Characterization of microbial activity

Bacterial production, respiration, and growth efficiency were calculated following Ward and Cory (2015). The average number of cells produced per day was calculated by subtracting initial cell concentrations from final cell concentrations, and then dividing this number by days of incubation. Paired t-tests were conducted with R (R Core Team, 2013) to determine statistical significance between treatments for bacterial respiration, production, growth efficiency, and number of new cells produced per day ($\alpha = 0.05$).

2.4.3. Metatranscriptomics of microbial communities

RNA sequences were trimmed, quality-controlled, and assembled by the Joint Genome Institute's assembly team. Raw reads were first quality-trimmed to Q10 and adapter-trimmed using BBDuk (Bushnell, 2015; options: ktrim=r, k=25, mink=12, tpe=t, tbo=t, qtrim=r, trimq=10, maq=10, maxns=3, minlen=50). Reads were then filtered for process artifacts using BBDuk (options: k=16). Ribosomal RNA reads were removed with BBMap (Bushnell, 2015) by mapping against a trimmed version of the Silva 119 database (options: fast=t minid=0.90 local=t). BBMap was also used to remove human reads. Metatranscriptomes were assembled with trimmed and quality controlled reads using MEGAHIT (Li et al., 2015; version 0.2.0; options: --cpu-only -m 100e9 --k-max 123 -l 155).

Coding sequences (CDS) were then predicted from assemblies with Prodigal (Hyatt et al., 2010) and annotated to the Kyoto Encyclopedia of Genes and Genomes database (KEGG; Kanehisa & Goto, 2000) and a custom phylogenetic database, according to the Joint Genome Institute's Standard Operating Procedure (Huntemann et al., 2015). Bowtie 2 was used to map filtered nucleotide sequences to CDS (Langmead et al., 2012), and SAMtools was used to extract counts, CDS lengths, and alignment lengths from Bowtie 2 output (Li et al., 2009). A CDS received one count if either both ends or only one end of a paired-end read mapped to a CDS. All CDS annotated to the same KEGG ortholog group (KO) were then summed, and a KO abundance table was produced. Counts per annotation were normalized to transcripts per million (TPM; Wagner et al., 2012). Briefly, this normalization reduces biases associated with library size, CDS length, and read alignment length, and expresses all counts as a portion of one million, so the sum of counts in each library is one million.

Pairwise similarities among metatranscriptomes were calculated using Bray-Curtis similarity values (Legendre & Legendre, 1998) and visualized in non-metric multidimensional scaling space using the R packages vegan (Oksanen et al., 2007) and ggplot2 (Wickham, 2009). The difference between treatments was assessed with multivariate analysis of variance (MANOVA) and 95% confidence intervals measured by standard error using R packages vegan (Oksanen et al., 2007) and ellipse (Murdoch & Chow, 1996). Alpha

diversity of each metatranscriptome was quantified by the Shannon index. Similarity Percentage analysis (SIMPER) was carried out in PRIMER v6 & PERMANOVA+ (PRIMER-E Ltd., Plymouth, UK) to determine the percent contribution of each gene to differences between treatments. MEtaGenome ANalyzer (MEGAN; Huson et al., 2009) and ShotMAP (Nayfach et al., 2015) software were used to explore abundances of transcripts within KEGG categories, pathways, and individual KOs. Paired t-tests were conducted with R (R Core Team, 2013) to determine significant differences between categories, pathways and KOs ($\alpha = 0.05$).

To test several hypotheses, a number of gene categories were manually curated. These categories included aromatic degradation, which was simply the KEGG pathway for aromatic degradation, in addition to oxygenase and decarboxylase genes defined as KOs named “oxygenase” and “decarboxylase,” respectively. Transcript abundances of genes within each category were then expressed as percentages of total Metabolism expression (KEGG tier II category). A number of ATP Binding Cassette (ABC) transporter categories were also created, including categories for the transport of phosphorus, amino acids, peptides, sugars, polyols (alcohols with multiple hydroxyl groups; not including alcohols containing phosphate), and inorganic ions (all but phosphate). Genes within these categories were expressed as percentages of total ABC Transporter expression (KEGG tier IV pathway).

2.4.4. Microbial community composition

Amplicon sequences were paired using make.contigs (MOTHUR v.1.32.1; Schloss et al., 2009), and converted to QIIME format with split.groups from MOTHUR and add_qiime_labels.py from QIIME (Caporaso et al., 2010). Sequences were quality filtered with an expected error rate of 0.5, dereplicated (derep_fulllength), and abundance sorted (sortbysize) using USEARCH (v.7.0.1001_i86linux64; Edgar, 2013). Singleton sequences were removed in the latter step to prevent them from seeding clusters when clustering OTUs. Reads were then clustered (cluster_otus) at 97% similarity and chimeras were removed via the de novo chimera check inherent in the cluster_otus in addition to reference-based chimera filtering (uchime_ref) with the Gold Database (www.genomesonline.org) as reference. Reads (including singletons) were subsequently mapped back to OTUs using UPARSE (usearch_global) and an OTU table was created. Taxonomy of the representative sequences was assigned in QIIME (assign_taxonomy.py) using the RDP classifier trained to the SILVA database (v.111 database clustered to 97% OTUs). Dominant taxa associated with metatranscriptomes were classified to the phylum or class level for analysis. Taxa that did not make dominant contributions to the metatranscriptomes were classified as "other."

3. RESULTS

3.1. Effect of photochemical and biological degradation on DOM

Approximately 10% of DOM was consumed or altered during sunlight exposure. Sunlight converted 5.2 ± 0.5% of DOM to CO_2 and broke down higher molecular weight DOM into lower molecular weight DOM, as indicated by a decrease in the average mass of DOM chemical formulas detected by FT-ICR MS and an increase in slope ratio, an optical proxy for DOM molecular weight. The chromophoric and fluorescent fraction of DOM also decreased after sunlight exposure, as did the ratio of aromatic to aliphatic carbon atoms, according to ^{13}C NMR. Further, ^{13}C NMR reported DOM lost 2-3% of carboxyl carbon after sunlight exposure and consumed less than 1 mol of O_2 per mol of CO_2 produced.

FT-ICR MS indicated that the majority of DOM chemical formulas (69-79%) were common to dark-control and light-exposed treatments, but that sunlight exposure caused significant changes in the peak intensities of many of these formulas. Of the 1729 common peaks detected by FT-ICR MS, 375 were photo-degraded, or decreased in intensity during light exposure (by an average of 32%), while 784 were photo-produced, or increased in intensity during light exposure (by an average of 36%; Fig. 2). Photo-degraded formulas had lower H/C ratios and higher O/C ratios than photo-produced formulas, and many were classified as highly oxidized, tannin-like compounds (73%), aromatic compounds (37%), or both (Fig. 2). Sunlight may have also caused complete loss or production of a small number of formulas, but the

percent of common peaks across experimental replicates was similar to the percent of common peaks across instrumental replicates, making it difficult to discern which formulas were truly lost or produced versus which were present or absent due to instrumental error. Finally, unlike the humic DOM detected by FT-ICR MS, low molecular weight DOM was not significantly changed by photo-exposure according to Orbitrap MS.

Similar to photo-exposure, 5 d incubations of bacteria with dark-control DOM also caused changes to the distribution (peak intensity) of many DOM formulas, although these changes were not significant. Additionally, there was overall strong overlap in the composition of formulas degraded by sunlight and formulas degraded by bacteria (Fig. 2). Of the 1871 peaks detected, 383 peaks were biologically degraded, or decreased in peak intensity during the incubation. Like photo-degraded formulas, many bio-degraded formulas were classified as highly oxidized, tannin-like compounds (64%), aromatic compounds (39%), or both. In fact, 39% of bio-degraded formulas shared exact masses with photo-degraded formulas. Furthermore, bio-degraded and photo-degraded formulas had similar molecular masses, O/C ratios and H/C ratios, and these characteristics were distinct from those of photo-produced formulas. Bio- and photo-degraded formulas had average molecular masses of 539 Da and 566 Da, average O/C ratios of 0.61 and 0.64, and average H/C ratios of 0.90 and 0.88, respectively. In contrast, photo-produced formulas had an average molecular mass of 460 Da, an average O/C ratio of 0.52 and an average H/C ratio of 1.02. However there was some overlap between bio-

degraded and photo-produced formulas, including 12% of bio-degraded formulas that shared exact masses with photo-produced formulas (Fig. 2).

3.2. Global response of microbial communities to DOM source

All measures of microbial activity were lower in the light-exposed treatment at or after 5 d of incubation, including respiration (O_2 consumption and CO_2 production), biomass production, new cell production, and growth efficiency (Fig. 3), although these differences were not statistically significant.

Gene expression patterns, measured after 4 h of incubation, also differed between treatments. Metatranscriptomes annotated to the KEGG database clustered separately on a non-metric multidimensional scaling diagram created with Bray-Curtis similarity values (MANOVA, $p = 0.1$), and 95% confidence intervals for each treatment, did not overlap (Fig. 4a). Replicate metatranscriptomes were also more variable in the light treatment, with an average Bray-Curtis similarity of 79% compared to 88% in the dark (Fig. 4a). The light treatment also had significantly lower Shannon index alpha diversity (Fig. 4b; paired t-test, $p \leq 0.05$).

Across metatranscriptomes, relative transcript abundance of KEGG ortholog groups (KOs), from here on referred to as genes, ranged several orders of magnitude, from 0 to over 24,000 TPM (Fig. 4c). Although many transcripts were found in similar abundance in light and dark treatments, discrepancies in the levels of certain highly expressed genes contributed to differences in metatranscriptome clustering (Fig. 4c). A Similarity Percentages analysis (SIMPER) determined that the 43 genes with the highest percent-

contribution to dissimilarity were cumulatively responsible for 30% of dissimilarity between treatments (Fig. 4c). Of these 43 top contributors to dissimilarity, 34 were more expressed in the light treatment while 9 were more expressed in the dark control. Twenty-nine of the 34 genes more abundant in the light treatment were involved in translation, and coded for ribosomal proteins, RNA polymerase, and elongation factors. These genes cumulatively contributed to 19% of dissimilarity. Of the 9 top contributors to dissimilarity that were more expressed in the dark, several were involved in motility and transport, such as flagellin, a methyl-accepting chemotaxis protein, two porins, and a component of a transporter for siderophore-iron complexes.

Across the 9,021 genes detected in the experiment, transcript abundance of 1,434 was significantly different between treatments (paired t-test; $p \leq 0.05$), as were sums of transcript abundance for genes composing certain KEGG categories. KEGG's tier II categories give a general overview of the differences observed between treatments (Fig. 5a). Summed transcript abundance for KEGG's tier II category, Genetic Information Processing, was significantly greater in the light-exposed treatment, while abundances for tier II categories Metabolism, Environmental Information Processing, and Cellular Processes were significantly greater in the dark control (Fig. 5a; paired t-test, $p \leq 0.05$).

In the light-exposed treatments, higher expression of genetic information processing genes was largely explained by significantly higher abundance of transcripts involved in transcription and translation (Fig 5b;

paired t-test, $p \leq 0.05$). In particular, expression of RNA polymerase and ribosomal proteins was significantly higher in the light (paired t-test, $p \leq 0.05$). Not all categories in Genetic Information Processing were higher in the light, however. Replication and Repair was the only category within Genetic Information Processing with elevated expression in the dark, though not significantly. Aminoacyl tRNA Synthesis, which falls under Translation, was also elevated in the dark control, but again not significantly (Fig. 5b).

In the dark-control treatments, higher expression was detected in a wide variety of categories that fell under Metabolism, Environmental Information Processing, and Cellular Processes. All types of metabolism, except nucleotide metabolism, were more expressed in the dark-control, including carbohydrate, amino acid, lipid, and xenobiotic metabolism, which were all significantly higher in the dark (Fig 5c; paired t-test, $p \leq 0.05$). Higher expression in Environmental Information Processing was mostly due to significantly higher abundance of signal transduction transcripts (Fig. 5d; paired t-test, $p \leq 0.05$), particularly transcripts for two-component systems (paired t-test, $p \leq 0.05$). Highly expressed two-component system genes included those encoding a methyl-accepting chemotaxis protein, a pilus assembly protein, and flagellin, which were highly expressed in both treatments but significantly more expressed in the dark control (paired t-test, $p \leq 0.05$). Glutamine synthetase and a phosphate transport system substrate binding protein were also highly expressed in both treatments, and more expressed in the dark-control, though not significantly. The number of

transcripts associated with membrane transport, which were mostly for ABC transport, did not differ significantly between treatments, although the distribution of individual transporter expression did (Fig. 5d). Finally, transcript counts in the Cellular Processes category were higher in the dark-control largely due to enrichment of cell motility transcripts (paired t-test, $p \leq 0.05$), such as transcripts for flagellar assembly and chemotaxis (paired t-test, $p \leq 0.05$; Fig. 5e). The number of transcripts involved in cell growth and death was also significantly higher in the dark control (paired t-test, $p \leq 0.05$), including genes for the cell division protein FtsW and for two Clp proteases (Fig. 5e).

3.3. Genetic evidence for sunlight's effect on DOM

Relative expression of select groups of enzymes and transporters was investigated to yield inference about how sunlight affects DOM chemistry. These groups of genes were expressed as percentages of appropriate categories. Decarboxylases, oxygenases, and genes involved in aromatic degradation were expressed as percentages of total metabolism expression, and the sums of each group made up larger percentages of metabolism in the dark-control. In fact, percent of both oxygenase and aromatic degradation transcripts almost doubled from dark to light treatment. Additionally, all significantly differentially expressed genes in these three categories were more expressed in the dark control, except one (Fig. 6a; paired t-test, $p \leq 0.05$). Many of the genes with significantly higher expression in the dark control were involved in the oxidation and cleavage of aromatic rings, such as

catechol 1,2-dioxygenase, catechol 2,3-dioxygenase, vanillate monooxygenase, phthalate 4,5-dioxygenase, homogentisate 1,2-dioxygenase, phenol hydroxylase, and salicylate hydroxylase (Fig. 6a).

Transporters were also investigated to determine how exposure to sunlight may have affected DOM, since transporter expression levels can suggest the types of organic matter and nutrients available to cells (Poretsky et al. 2010, McCarren et al. 2010). Because most transporter expression was for ABC transporters, we focused on these, and expressed transcript abundance for each ABC transporter gene as a percentage of total ABC transporter expression, despite that total ABC transporter expression was similar across treatments (paired t-test, $p > 0.05$).

There were 355 ABC transporter genes detected across treatments, including transporters for phosphorus and nitrogen sources, sugars, polyols (alcohols with multiple hydroxyl groups), and inorganic ions. Forty genes in these categories, representing subunits for 24 transporters, demonstrated significantly different expression across treatments (Fig. 6b). Of these 40 genes, 9 were more expressed in the light treatment (representing 5 transporters) while 31 were more expressed in the dark treatment (representing 19 transporters).

Transcripts associated with phosphorus transport were by far the most abundant in both treatments, but while the transporter for phosphate was more expressed in the dark control, transporters for sn-glycerol 3-phosphate and phosphonate were more expressed in the light treatment (Fig. 6b). In

total, phosphorus transport in the light treatment averaged 66% of ABC transport expression compared to 50% in the dark, but this difference was not significant (paired t-test, $p = 0.11$)

Expression for nitrogen source transport was also substantial. Amino acid transport gene expression comprised 18% of ABC transport in the dark and 9% in the light (paired t-test, $p \leq 0.05$). Ten of the 66 genes for amino acid transporters demonstrated significantly different expression between treatments (paired t-test, $p \leq 0.05$), five of which had higher expression in the light treatment and five of which had higher expression in the dark control (Fig. 6b). The five genes with higher light-treatment expression encoded components of cystine, methionine, and arginine transporters, while the five genes with higher dark-control expression encoded components of general L-amino acid, branched-chain amino acid, histidine, and lysine/arginine/ornithine transporters (Fig. 6b). Similar to amino acid transport, total peptide transporter expression was significantly higher in the dark control, making up 3% of ABC transport compared to 2% in the light treatment (paired t-test, $p \leq 0.05$). However, expression patterns of individual transporters were highly variable.

Transporters for sugars and polyols were consistently higher in the dark control. Total sugar transport was responsible for 8% of ABC transport in the dark control and 5% in the light treatment, while total alcohol transport made up 0.93% of ABC transport in the dark control and 0.21% in the light treatment (the alcohol transport category did not include genes for transport

of the phosphate-containing alcohols, sn-glycerol 3-phosphate and inositol-phosphate, which were more expressed in the light). Furthermore, all 10 and 11 differentially expressed sugar and alcohol transport genes, respectively, had greater expression in the dark (Fig. 6b; paired t-test, $p \leq 0.05$).

Expression for total inorganic ion transport averaged 5% of ABC transport in the light treatment and 3% in the dark, and the five genes in this category that showed significantly different expression were all more expressed in the dark (Fig. 6b). These five genes encoded two components of a molybdenum transporter, and components of sodium, cobalt/nickel and siderophore-complexed iron transporters. There were, however, several inorganic ion transporters that displayed higher expression in the light treatment for each replicate, but due to high variability these differences were not statistically significant. For example, in contrast to higher expression of the siderophore-complexed iron transporter in the dark control, there was higher expression of the free iron(III) transporter in the light treatment, with the sum of all components averaging 3.03% of ABC transport in the light and 0.91% in the dark (paired t-test, $p = 0.25$). The sulfate transporter also demonstrated higher expression in the light for each replicate (paired t-test, $p = 0.16$).

3.4. Taxonomic response to DOM source

All taxa composing light and dark communities at 4 h were identified using 16S ribosomal RNA amplicon sequencing, and though not identical, community composition was very similar between treatments (Fig. 7). In both

light and dark treatments, Gammproteobacteria dominated, comprising about 45% of the community. Alphaproteobacteria, Betaproteobacteria, and Bacteroidetes also made up substantial portions of the communities in both treatments (between 4 and 14%), but both Alphaproteobacteria and Betaproteobacteria were more abundant in the light treatment, whereas Bacteroidetes were more abundant in the dark. Actinobacteria, Acidobacteria and Firmicutes each made up less than 10% of the communities, but Acidobacteria and Firmicutes were both slightly more abundant in the dark treatment. Bacteria categorized as “other” also made up almost 20% of the taxa present, 7% of which was made up of Verrucomicrobia in both treatments.

The composition of taxa associated with metatranscriptomes was evaluated by assigning taxonomy to transcripts, and was not only distinct from the composition of the entire community (16S-determined), but also demonstrated more pronounced differences between treatments (Fig. 7). For example, transcripts associated with Gammaproteobacteria were dominant in both treatments, but whereas in both treatments this class comprised about 45% of the community (based on 16S amplicon sequencing), it contributed 57% of transcripts in the light treatment and 35% in the dark. Betaproteobacteria and Bacteroidetes were also well represented in the metatranscriptomes, but in contrast to Gammaproteobacteria, contributed more transcripts in the dark treatment relative to abundance. Alphaproteobacteria, Acidobacteria, Actinobacteria, and Firmicutes were also

represented to a lesser extent in the metatranscriptomes, and also contributed a higher proportion of transcripts relative to their abundances in the dark treatment. Finally, “other” bacteria were poorly represented in the metatranscriptome relative to their abundances (less than 5% of metatranscriptome-associated taxa compared to almost 20% of 16S-associated taxa). Verrucomicrobia, which was categorized as “other,” contributed to less than 1% of transcripts.

The taxa responsible for the expression of specific KEGG pathways, including Ribosome, DNA Replication, and TCA Cycle pathways, were similar in composition to taxa responsible for all expression (Fig. 7). The same taxa dominated each pathway, especially Gammaproteobaceria, Bacteroidetes and Betaproteobacteria, and the same shifts occurred from dark to light treatment. For example, Bacteroidetes supplied a greater number of transcripts for these pathways in the dark control while Gammaproteobacteria supplied a greater number in the light treatment. Subtle differences between expression of pathways were apparent, however. For example, Gamma- and Beta-proteobacteria dominated transcription of the light treatment’s ribosomal genes to an even larger degree than they dominated other pathways in the light or dark treatment, together contributing over 90% of ribosomal transcripts.

The composition of taxa expressing genes for aromatic degradation was distinct from that of other pathways in that the relative abundances of taxa was strikingly similar between light and dark treatments.

Gammaproteobacteria made up roughly 60% of the community in both light and dark treatments, and even contributed a slightly greater proportion of transcripts in the dark, unlike for any other pathway. Betaproteobacteria, Alphaproteobacteria, and Bacteroidetes contributed most of the remaining transcripts.

4. DISCUSSION

Our results demonstrate that even small amounts of sunlight have the capacity to alter DOM in ways that evoke profound changes in its metabolism by microbes. Not only are rates of microbial metabolism altered after DOM has been exposed to sunlight, but microbial gene expression, and the taxonomic groups conducting this expression, are altered too. We also provide evidence that this effect is likely caused by sunlight's removal of labile DOM. Finally, by comparing the gene expression of microbial communities metabolizing light-exposed and dark-control DOM, we generated both insight and new hypotheses about the mechanisms by which sunlight affects DOM chemistry and evokes a biological response.

4.1. Effect of photochemical and biological degradation on DOM

It is clear that even a short-term exposure to sunlight can affect substantial change on the chemical composition of DOM (Fig. 2). If 10% of DOM formulas were consumed or altered in this short-term experimental exposure, then sunlight likely plays a large role in altering DOM in natural freshwaters, both in the Arctic (Cory et al., 2014) and globally (Koehler et al., 2014).

Photo-exposure altered the chemical composition of DOM in several ways. First, sunlight converted larger, more aromatic compounds into smaller, less aromatic compounds, as evidenced by decreased molecular weight, increased H/C, loss of chromophoric and fluorescent fractions, and decreased

aromatic to aliphatic carbon ratio. This is consistent with earlier studies showing that sunlight decreases aromatic character of DOM and reduces molecular weight (Hudson et al., 2007; Moran et al., 2000; Strome & Miller, 1978; Wetzel et al., 1995). FT-ICR MS also identified changes in the molecular signature of DOM (i.e., increase in H/C, decrease in O/C) that were consistent with other studies (D'Andrilli et al., 2015; Gonsior et al., 2013; Gonsior et al., 2009; Gonsior et al., 2014; Stubbins et al., 2010). The increase in H/C suggests DOM became less condensed (aromatic) after sunlight exposure, which was expected and confirmed by several other methodologies mentioned above. While a decrease in O/C would ordinarily suggest DOM became less oxidized, there are multiple lines of evidence that DOM actually became more oxidized, and that instrumental limitations of FT-ICR MS explain why highly oxidized compounds were not detected. This explanation is given in more detail in Ward & Cory (2016), but briefly, photo-exposure likely led to the formation of compounds that do not ionize well and are therefore not detected during mass spectrometry. These compounds are likely highly oxidized carbohydrate-like compounds (C. Ward, pers. comm.).

While aromatic degradation and oxidation of DOM are well-established results of photo-exposure, less established is the idea that sunlight decarboxylates DOM, or removes carboxyl groups. Although photo-decarboxylation has been proposed as a primary pathway for the degradation of DOM for many years (Miles & Brezonik, 1981), few have provided evidence. Here however, several pieces of evidence, which are outlined in

more detail in Ward & Cory (2016), point to decarboxylation. First, 2-3% of carboxyl carbon was lost after photo-exposure, suggesting decarboxylation provided a major avenue of DOM mineralization to CO_2. O_2 and CO_2 were also consumed and produced, respectively, in the proportions expected if decarboxylation were a major pathway for degradation of DOM (less than 1 mol of O_2 produced per mol of CO_2 consumed). Finally, the H/C ratio of DOM formulas decreased, which is an expected result of decarboxylation.

Overlap of photo-degraded and bio-degraded formulas identified by the FT-ICR MS strongly suggests that light exposure removed compounds labile to bacteria. Not only were 39% of photo-degraded formulas identical to bio-degraded formulas, but photo- and bio-degraded formulas had similar average molecular mass, similar H/C and O/C ratios, and the majority of formulas in both groups were classified as highly-oxidized tannin-like compounds. It is true that identical molecular formulas do not imply identical molecular structure, and that isomers can have very different reactivities, but the chances for “competition” between sunlight and microbes are surely increased when both degrade compounds with similar character.

FT-ICR MS results also indicated that aromatic compounds made up a sizeable fraction of the DOM susceptible to both photochemical and biological degradation. Aromatics have been called the most photo-reactive fraction of the DOM pool (Stubbins et al., 2010), but have never been regarded as the most bioreactive fraction. However, the biological degradation of aromatics observed here is consistent with recent indications that labile DOM must

consist of more than just low molecular weight, nitrogen-rich compounds (Frazier et al., 2005; Mann et al., 2012; Sleighter et al., 2014; Volk et al., 1997; Ward et al., 2013; Wetzel, 2003). While low molecular weight compounds may be the most labile fraction of DOM, mass balance demonstrates that humic, aromatic carbon compounds must make up the majority of biodegraded DOM (Cory & Kaplan, 2012). Also reflective of the importance of aromatic degradation to microbial metabolism in many environments are the multiple pathways for aromatic degradation that bacteria have evolved (Fuchs et al., 2011) and the extensive diversity of aromatic degradation genes (Iwai S, et al. 2010). So if aromatic compounds comprise a readily bioavailable fraction of DOM, as recent evidence suggests, the degradation of these compounds by both photochemical and biological processes again suggests “competition” for these compounds.

Lastly, it cannot be overlooked that although sunlight degraded 39% of bio-degraded formulas, it also produced 12% of bio-degraded formulas. This suggests that although sunlight caused a net removal of bio-available compounds, it also produced some new labile compounds.

4.2. Global response of microbial communities to DOM source

All measurements of microbial activity after 5 d of incubation show that exposure of DOM to sunlight caused lower activity of microbial communities (Fig. 3). Not only were respiration, biomass production, and average new cell production lower in the light treatment, but growth efficiency was as well,

suggesting DOM in the light treatment was of lower quality than DOM in the dark control.

Numerous studies have found light exposure of DOM can lower microbial activity, and many have speculated that the removal of labile compounds by sunlight explains these results (Abboudi et al., 2008; Amado et al., 2014; Benner & Biddanda, 1998; Cory et al., 2013; Judd et al., 2007; Obernosterer et al., 1999; Tranvik & Bertilsson, 2001; Vallieres et al., 2008). But none of these studies provided direct evidence for how this happens. Here we present the first direct evidence to support this hypothesis. FT-ICR MS data indicate that lower activity of microbial communities after DOM photo-exposure occurs when sunlight removes a large fraction of the DOM compounds that microbes metabolized in the dark.

Previous studies show that sunlight's effect on DOM is enigmatic, sometimes reducing and sometimes enhancing lability depending on the DOM source and the degree of sunlight exposure (Abboudi et al., 2008; Amado et al., 2014; Benner & Biddanda, 1998; Cory et al., 2013; Judd et al., 2007; Obernosterer et al., 1999; Tranvik & Bertilsson, 2001; Vallieres et al., 2008). Studies examining these contrasting effects cover a variety of DOM sources and exposure times, but some of the most comparable to our study were consistent with our findings. Judd et al. (2007) found that photo-exposure of organic mat DOM from birch-willow tundra (the same type of DOM that our study used) caused microbial biomass production to decrease. DOM from Cory et al. (2013)'s "reference sites" was also comparable to DOM

from our study and consistent with our findings. Cory et al. (2013) found that DOM draining arctic sites of permafrost thaw became more labile after 24 h sunlight exposure, while DOM draining reference sites, i.e., DOM from waters absent of permafrost thaw, generally became less labile. Because the hydrologic flow through soil draining reference sites did not penetrate much below the organic mat, this DOM was likely similar to DOM from our study. Taking our FT-ICR MS data into account, it is probable that the effects of sunlight on organic mat DOM analyzed in Judd et al. (2007) and Cory et al. (2013) were due to the photo-consumption of labile compounds. It is also probable that contrasting effects observed in other studies can be attributed to the photo-consumption or photo-production of labile compounds, depending on the effect. It should be noted, however, that sunlight will both produce and consume labile compounds, as it did in this experiment, but the net production or consumption of labile compounds will likely be a large factor in determining activity of microbial communities.

In addition to changing rates of microbial activity, exposing DOM to sunlight led to dramatic shifts in microbial gene expression after just 4 h, as indicated by the clustering of metatranscriptomes by treatment, differences in Shannon alpha diversity, and differential expression of many genes and gene categories (Figs. 4 & 5). The inoculum microbial community was adapted to using dark-control compounds, many of which were likely removed by sunlight. Thus, if light treatment communities were to instead use photo-exposed DOM, they had to initiate the appropriate modifications in gene

expression. Transcriptional responses to resource changes have been observed in the past (de Menezes et al., 2012; McCarren et al., 2010; Poretsky et al., 2010; Shi et al., 2012; Teeling et al., 2012), but transcriptional responses in this experiment highlight the large impact that a small amount of DOM photo-exposure can have on microbial metabolism. Sunlight altered only about 10% of DOM, but the 10% it altered was microbially relevant. These results support the idea that sunlight is a key element determining the microbial processing of DOM in natural waters (5).

Global shifts in gene expression, measured after 4 h, clearly indicate that sunlight altered a fraction of DOM that was important to microbial communities. The most striking difference between treatments was elevated transcription and translation gene expression in response to light-treated DOM, and elevated metabolism, motility, and transport gene expression in response to dark-control DOM. Elevated transcription and translation are generally interpreted as signs of microbes entering lag or log growth phases (Kraakman et al., 1993; Madar et al., 2013; Nomura et al., 1984; Rolfe et al., 2011), likely in response to a change in growth conditions like the ones experienced by light treatment communities. This is because cells tightly regulate ribosome biosynthesis and generally allocate more resources to ribosomes and other cellular machinery involved in protein synthesis when their growth rates are higher (Scott et al., 2010). However, light treatment communities also displayed reduced expression of genes for other growth indicators including DNA replication and the TCA cycle (Chang et al., 2002;

Clark et al., 2006). For dark control incubations, elevated metabolism, motility, transport indicate growth in sub-optimal conditions, which is consistent with the relatively low quality of soil-derived DOM for bacterial growth (Pérez & Sommaruga, 2006). Cells tend to allocate more energy to moving and scavenging when resources are scarce (Soutourina & Bertin, 2003), suggesting that resources were scarce in the dark treatment and probably prohibitive of rapid growth. These results suggest DOM photo-products caused the inoculum microbial community to shift from slow growth to lag or log phase. Interestingly, this initial shift in growth phase did not result in higher growth rates or greater cell production over the 5 d incubation, suggesting that lag phase was ongoing at 5 d, or photo-exposure of DOM caused transient log growth that ended before 5 d.

Several pieces of evidence support the idea that the light treatment community was undergoing lag phase at 4 h, explaining lower growth over the 5 d incubation. The lag phase, or the initial period in the bacterial growth cycle when no growth is observed, takes place when cells encounter new environmental conditions and must adjust metabolism accordingly (Madar et al. 2013; Monod, 1949). Although communities in both treatments encountered new conditions by being diluted at the beginning of incubations, conditions were newer for light treatment communities because the common inoculum had been growing with dark-control DOM. Therefore it is possible that the lag phase was short or non-existent in the dark treatment, since cells in this treatment were already adjusted to dark-control DOM. Gene

expression of the light treatment communities is also consistent with our limited knowledge of lag phase expression patterns (Schultz & Kishony, 2013). In one of the few studies of lag phase gene expression, Rolfe et al. (2011), studying cultures of *Salmonella enterica,* found upregulation of genes encoding RNA polymerase and ribosomal proteins. In fact, the core subunits of RNA polymerase reached peak expression during lag phase, while ribosomal protein expression was high until mid-exponential phase, suggesting synthesis of transcription and translation machinery is a prerequisite for exponential growth. Interestingly, Madar et al. (2013) found that only when cells began to grow in size were ribosomal promoters activated, so perhaps the light treatment communities had embarked on this part of the lag phase. Also consistent with light treatment gene expression, Rolfe et al. (2011) found that during lag phase, phosphorus and iron(III) uptake were upregulated, while genes for the transport of molybdenum, cobalt and nickel and for the TCA cycle were downregulated. Although expression during lag phase is not well understood, the similarity between lag phase expression in prior studies and expression in the light treatment suggests lag phase may explain the light treatment's high expression for transcription and translation pathways, despite minimal growth after 5 d. In addition, it would reconcile the apparent inconsistency of the light treatment's reduced expression for DNA replication and TCA cycle genes.

Another likely explanation for expression and activity patterns is that a brief spurt of logarithmic growth was occurring in the light treatment at 4 h, but

that this growth was followed by stationary phase or even cell death that explains lower activity over 5 d. This could have happened if photo-exposure of DOM produced highly labile compounds or nutrients that initially enhanced growth, but became depleted before 5 d. In fact, FT-ICR MS indicated that 12% of bio-degraded formulas were produced by sunlight, some of which could have been responsible for enhanced growth. It is also possible that sunlight produced low molecular weight labile compounds, too small to be detected by the FT-ICR MS (Moran & Zepp, 1997). However, the low molecular weight formulas detected with Orbitrap MS had similar peak intensities before and after photo-exposure, suggesting that new low molecular weight compounds were not produced. Photochemical release of nutrients from DOM could also explain initial logarithmic growth in the light treatment, but lower growth at 5 d. Humic acids, which make up the majority of soil DOM, form complexes with ions and create humic colloids, altering the bioavailability of these ions (Wershaw, 1989). Sunlight exposure has been known to release organically complexed metals, nitrogen, and phosphorus (Bushaw et al., 1996; Francko & Heath, 1982; Shiller et al., 2006; Vähätalo et al., 2003), and could have allowed nutrient uptake and growth by the light treatment communities until depletion or re-complexation. In fact, Vähätalo et al. (2003) demonstrated that this kind nutrient release and depletion could take place on the timescales of this experiment. Investigating photochemical transformation of DOM from a humic lake, Vähätalo et al. (2003) found that concentrations of phosphate increased after photo-exposure, causing

phosphatase levels of microbial incubations with this DOM to decrease relative to dark controls. However, after 4 d of incubation, these same microbial communities produced more phosphatase than dark-control DOM. Something very similar could have occurred in this experiment, in which an initial photochemically induced pulse of phosphorus triggered growth in the light treatment, but soon light communities were even more phosphorus limited than dark-control communities.

Global shifts in gene expression in this experiment demonstrate that even slight photo-alteration of DOM can elicit profound effects on microbial community functioning. Interpretation of these shifts is challenging, however, because most gene expression studies involve model organisms grown at optimal conditions in the laboratory, and because studies that examine community gene expression rarely include any direct measurements of growth. Regardless, transcriptional responses in this experiment suggest that DOM photo-alteration elicits transcriptional responses in natural waters too. Thus natural variability in photo-alteration of DOM could lead to frequent shifts in growth phases of microbial communities or populations. Perhaps DOM photo-alteration could even play a role in the diel cycles of microbial expression patterns in sunlit waters (Hewson et al., 2010). It is clear that photo-exposure of DOM causes global changes in microbial expression patterns, which likely lead to changes in activity and carbon processing. When scaled up, these changes likely have profound effects on the elemental cycling of ecosystems.

4.3. Genetic evidence for sunlight's effect on DOM

In addition to investigating global expression patterns across treatments, we interrogated the dataset to test specific hypotheses about how sunlight affects DOM. Because microorganisms are extremely sensitive to changes in their environment, metatranscriptomics can be used as a sensitive tool to detect changes in DOM (de Menezes et al., 2012; McCarren et al., 2010; Poretsky et al., 2010; Shi et al., 2012; Teeling et al., 2012), complimenting analytical techniques. Here, not only does metatranscriptomics provide new lines of evidence to substantiate data produced by analytical techniques, but it also allows for the generation of new hypotheses, which can in turn be tested by analytical techniques.

We first tested if sunlight degraded aromatic compounds or oxidized DOM, replacing the function of genes that ordinarily carry out these processes. Lower expression of the aromatic degradation pathway and oxygenases in the light treatment suggests that sunlight did both. The degradation of aromatics by sunlight is consistent with analytical measures from this experiment and others (Hudson et al., 2007; Moran et al., 2000; Opsahl & Benner, 1998; Scheck & Frimmel, 1995; Strome & Miller, 1978; Stubbins et al., 2010). Likewise, the response of microbial communities to this degradation is consistent with prior work. To break down aromatics, microbes use energetically costly enzymes such as oxygenases, peroxidases and laccases to hydroxylate and cleave aromatic rings (Bugg et al., 2011; Fuchs et al., 2011; Gulvik & Buchan, 2013). It is thought that sunlight instigates the

same processes through the formation of reactive oxygen species (Cory et al., 2010). In this way, photo-exposure of DOM could have replaced the function of oxygenases and other costly enzymes involved in aromatic degradation, reducing the need for expression of these genes. This reduced need for oxygenase expression also suggests photo-oxidation of DOM in addition to photo-degradation of aromatics. Oxygenases incorporate molecular oxygen into DOM and are important to a range of cellular reactions besides aromatic degradation. Thus lower oxygenase expression in the light treatment suggests sunlight oxidized DOM in place of oxygenases. Photochemical oxidation of DOM is also supported by the production of radical oxygen species upon DOM's exposure to sunlight (Page et al., 2014) and has been demonstrated using $^{18}O_2$ (Cory et al., 2010), FT-ICR MS (Gonsior et al., 2009; Kujawinski et al., 2004) and NMR spectroscopy (Schmitt-Kopplin et al., 1998). Here metatranscriptomics provides another line of evidence for such photochemical processes and simultaneously demonstrates a microbial response.

We also tested the hypothesis that photo-decarboxylation, or the photochemical removal of carboxyl groups from DOM, was an important mechanism by which DOM was photo-degraded. Lower expression of decarboxylases in the light-exposed treatment supports this hypothesis, suggesting that microbial communities had less of a need to decarboxylate DOM because sunlight had already done so. In contrast to aromatic degradation and oxidation, decarboxylation of DOM by sunlight is not well

documented. Photo-decarboxylation mechanisms have been identified, and it has been suggested a major pathway for the photochemical production of CO_2 (reviewed by Mopper et al., 2014), but evidence has been difficult to produce. For example, one study found no correlation between photochemical CO_2 production and DOM carboxyl content (Anesio et al., 2005), although this may be explained by the regeneration of carboxyl groups during photo-decarboxylation (Xie et al., 2004). Recently some of the strongest chemical evidence for decarboxylation emerged (Ward & Cory, 2016), and here metatranscriptomics provides new biological evidence for photo-decarboxylation.

Differences in expression of transporters were also used to address hypotheses about sunlight's effect on DOM. Taken together, shifts in transporter expression are yet another indication that sunlight altered a fraction of DOM relevant to microbial functioning. This is not the first time that changes in transporter expression have been detected in response to changes in DOM (e.g., Poretsky et al., 2010), but here, shifts in transporter expression allow insight into potential mechanisms of DOM photo-alteration.

The most highly expressed transporter was the phosphate transport system, which as its name suggests, transports orthophosphate, and alone represented 31% of ABC transport expression in the light treatment and 36% in the dark-control. High expression of phosphorus transporters in both treatments highlights the biological importance and the scarcity of this nutrient. However, higher expression in the dark treatment suggests microbial

communities in this treatment were more phosphate limited, since expression of this transport system increases upon phosphate starvation (Ishige et al., 2003). Sunlight has been shown to release phosphate from humic DOM in some systems (Cotner & Heath, 1990; Francko & Heath, 1982; Vähätalo et al., 2003; Zhang et al., 2013), but not in others (Gobler et al., 1997; Jorgensen et al., 1998; McCallister et al., 2005; Wiegner & Seitzinger, 2001). The mechanisms of this process are poorly understood (Francko, 1990; Mopper et al., 2014), but are thought to occur through the photo-reduction of iron, which often binds phosphate to iron-humic complexes (Francko & Heath, 1982). Here, reduced expression of phosphate transporters in the light treatment suggests that phosphate was released by sunlight.

Reduced phosphate transporter expression in the light treatment was coupled with increased expression of organophosphate transport. Organophosphates serve diverse cellular functions, and uptake may be preferable (with respect to inorganic phosphate) for cells carrying out certain functions. For example, synthesis of sn-glycerol 3-phosphate is the first step in the pathway for biosynthesis of phospholipid membranes (Cronan & Rock, 2008) and is probably less costly to import than synthesize (Ames, 1986). By this logic, if sunlight removed organophosphates by cleaving phosphate groups from their organic counterparts, transporters for organophosphates would be more highly expressed in the light treatment.

It is also possible that DOM chemistry was less of a factor in determining patterns of phosphorus transport expression than were biological

differences between the treatments. Thus findings may suggest photochemical release of phosphate from DOM, but they also suggest differences in the dominant metabolic processes taking place in each treatment. For example, it is possible that light treatment communities were building more phospholipids for cell membranes, and this too could explain higher expression for organophosphate transporters in the light treatment (Cronan & Rock, 2008). In fact, expression of total phosphorus transport (inorganic and organic), which was higher in the light, was likely a result of biological rather than chemical differences between treatments. Ribosomes demand a great deal of phosphorus (Merchant & Helmann, 2012), and light treatment expression for ribosome biosynthesis was about twice as high as it was in the dark treatment. This greater metabolic demand for phosphorus in the light treatment may reconcile higher total phosphorus transport in the light treatment despite indications that phosphate limitation was greater in the dark.

Expression of amino acid and peptide transport, if examined with the same logic as phosphorus transport, suggests photo-exposure of DOM may have increased nitrogen availability as well. Although not every transporter followed this pattern, amino acid and peptide transporters were generally more expressed in the dark control, suggesting more limitation than in the light treatment. Relatively little is known about the photochemical transformations of nitrogen species, and photoreactions may act as both sources and sinks for nitrogen, depending on several factors (Mopper et al.,

2014). Nonetheless many studies have reported increases in free amino acids after DOM photo-exposure, including several that involved humic DOM (Amador et al., 1989; Bushaw-Newton & Moran, 1999; Bushaw et al., 1996; Jorgensen et al., 1998). In fact, Amador et al. (1989) not only found that less glycine was bound to humic acids after photo-exposure, but subsequent biological incubations with photo-exposed and control DOM showed that 40-60% more glycine was metabolized in incubations with photo-exposed DOM. Although photochemical production of peptides is not as well documented as photochemical production of amino acids, a similar scenario could have taken place in our experiment, in which photo-exposure caused humic-bound nitrogen species to become unbound and bioavailable.

The exceptions to the amino acid transport trend were transporters of cystine, methionine, and arginine, which displayed higher expression in the light treatment rather than the dark control. Again a biological rather than photochemical explanation is possible here, especially considering the two amino acids containing sulfur, cystine and methionine, fell into this category. Based on high ribosomal expression, the cellular activities of the light treatment communities probably involved more protein synthesis than those in the dark control. Higher cystine and methionine transport could be explained by this process, since many proteins require sulfur-containing coenzymes (Sekowska et al., 2000). It is unclear why expression for arginine transport was higher in the light, but this particular amino acid could serve an important function in certain proteins being synthesized in the light treatment.

Transporters for sugars and polyols (alcohols with multiple hydroxyl groups) were all expressed more in the dark except for two transporters for phosphate-containing polyols, suggesting that sugars and polyols were limiting in the dark treatment, but became more available upon DOM photo-exposure. It is well known that photo-exposure of DOM can give rise to the production of labile, low molecular weight compounds, but production of low molecular weight acids, not sugars and alcohols, is often reported (Moran & Zepp, 1997). Gonsior et al. (2014) found that irradiation of refractory DOM produces polyols, so it is possible that sugars and alcohols are produced along with acids, but that acids are more easily detected.

Iron transporters for siderophore-complexed iron(III) were expressed more in the dark, while transporters for free iron(III) were expressed more in the light, suggesting a change in the source of available iron. Although prior interpretations of transporter expression have relied on the assumption that higher expression of a transporter suggests the substrate is more limiting, expression of these transporters can be interpreted differently, since both transporters use the same substrate, iron(III). Here, what likely determines higher expression of one transporter over the other is the requirement for siderophores, which are iron-scavenging molecules synthesized and secreted by microbes in iron limited conditions (Sandy & Butler, 2009). Therefore lower expression for siderophore-complexed iron(III) in the light treatment suggests that photo-exposure of DOM alleviated the need for iron scavenging.

Consistently, sunlight is known to break down iron(III)-DOM complexes and release free iron(III) (Voelker et al., 1997).

These findings highlight the usefulness of metatranscriptomic analysis in detecting changes in DOM that cannot be detected with current analytical techniques. In addition, using metatranscriptomics to investigate changes in DOM yields microbial-centric information about DOM, which is important if one is concerned with the photochemical effects on DOM's bioavailability and environmental cycling. Of course, metatranscriptomic data cannot provide conclusive evidence for any particular change in DOM, but it can provide new lines of evidence to support or contradict prior hypotheses, spark new hypotheses, and more broadly draw attention to the biological processes important in each community. Most importantly, the dramatic shifts in enzyme and transporter expression observed from dark to light treatment further indicate that a short-term exposure to sunlight can cause significant changes in DOM and its microbial processing.

4.4. Taxonomic response to DOM source

Community composition was similar between the two treatments, since DOM had been inoculated with the same microbial community. The small differences between the communities, however, can be explained by either of two scenarios. First, it is possible that a change in DOM caused community composition to shift over 4 h via rapid growth of certain taxa and death of others. Second, it is possible this change took place in DOM before inoculation, since production of DOM with a 0.45 μm filter did not entirely

sterilize DOM. Community composition of cells remaining in DOM may have diverged over the length of the photo-exposure.

Community composition included well-known soil and planktonic taxa (Crump et al., 2012; Janssen, 2006). The distribution of these taxa was not necessarily reflective of natural microbial communities, but this can almost certainly be attributed to the inevitable phylogenetic shifts that occur during confinement, due in part to faster growth of opportunistic populations and reduction of grazing pressure (Bouvier & Del Giorgio, 2007; Fuchs et al., 2000; Massana et al., 2001). This “bottle effect” may explain the dominance of Gammaproteobacteria, which often do well in confined experimental incubations (e.g., Fuchs et al., 2000) on account of having genomes well equipped for dynamic environments (Moran et al., 2007). Gammaproteobacteria are also well equipped for aromatic degradation (Moran et al., 2007), a seemingly large advantage during incubation with humic DOM. Other dominant taxa such as Alpha- and Beta-proteobacteria and Bacteroidetes are also commonly detected in incubations with aromatic carbon (Widada et al., 2002; Wu et al., 2008; Zocca et al., 2004). Change in community composition is a caveat of growing communities under batch growth conditions (Massana et al., 2001), and must be taken into account during analysis. However, the focus of this experiment was on function rather than phylogeny, so this caveat was accepted.

The composition of the whole community (16S amplicon sequencing) and the composition of active taxa (metatranscriptomes) were strikingly

different, as has been seen in many studies (e.g., Baldrian et al., 2012). Gamma- and Beta-proteobacteria and Bacteroidetes all made up larger portions of active taxa than the whole community, suggesting these taxa were growing more than other inoculum taxa. The relatively inactive taxa were likely not equipped to handle the conditions, and were instead dormant or slow-growing (Jones & Lennon, 2010; Kolter et al., 1993). It is also possible that database bias partly accounts for the lack of representation of certain taxa in metatranscriptomes. Taxonomic classification of metatranscriptomes relied on reference databases, in which the majority of sequences come from cultured organisms (Huson et al., 2009). This bias could explain why Verrucomicrobia, which are difficult to isolate (Sangwan et al., 2005), comprised 6% of the community, but less than 1% of the active taxa in both treatments.

The composition of active taxa differed between light and dark treatments, suggesting sunlight altered DOM in a way that favored certain taxa over others. The largest shift caused by DOM photo-exposure was an increase in expression by Gammaproteobacteria and a decrease in expression by Bacteroidetes. As mentioned, Gammaproteobacteria have genomes that confer advantages for a dynamic environment (Moran et al., 2007), which could have given them a competitive edge when incubated with an altered DOM source. Bacteroidetes are often considered specialists for the degradation of highly complex, high molecular weight organic matter (Thomas et al., 2011), partly because they possess an elaborate repertoire of hydrolytic

extracellular enzymes (Edwards et al., 2010; Gómez-Pereira et al., 2012). This may have given them an advantage in the dark treatment that was lost once sunlight converted high molecular weight DOM into smaller pieces. It is likely that differences in active taxa between treatments were at least partly driven by differences in the ability to process organic matter, once more underlining that biologically significant photo-alteration of DOM took place.

Taxonomic affiliations for expression of Ribosome, DNA Replication, and TCA Cycle pathways were generally quite similar to taxonomic affiliations for the entire metatranscriptome, suggesting that taxa were synthesizing ribosomal proteins, replicating, and respiring in roughly the same proportions. This was slightly truer of the dark treatment than the light treatment. In the light treatment, Gamma- and Beta-proteobacteria together contributed more than 90% of transcripts for ribosomal biosynthesis, suggesting these taxa were synthesizing relatively more ribosomes compared to other taxa. However, overall, taxonomic affiliations for these pathways were similar, as were differences between light and dark treatments.

In contrast, the Aromatic Degradation pathway did not demonstrate the same patterns. This pathway, made up primarily of transcripts associated with Gammaproteobacteria, followed by Betaproteobacteria, Alphaproteobacteria and Bacteroidetes, was expressed in remarkably similar proportions in the light and dark treatments. Seeing as the expression of other pathways demonstrated considerable taxonomic differences between treatments, one might predict that the Aromatic Degradation pathway would follow the same

trend. That it did not suggests that only a limited number of taxa are capable of aromatic degradation (Bugg et al., 2011), and that despite shifts in the taxa responsible for all expression, the aromatic degrading taxa remained fixed because no other taxa had the metabolic capability to take their place.

Further, it is intriguing that the aromatic degrading community looks strikingly similar to the light treatment community of other pathways. This is the opposite of what we expected, and it suggests that sunlight's destruction of aromatic compounds leads to an active community that is dominated by aromatic degrading organisms. However, it is more likely that a confounding factor is at play here. For instance, Gammaproteobacteria, which are dominant in both the aromatic degrading community and the active community, are capable of aromatic degradation, but also of rapid adjustment to new environments, and the latter could have been the actual cause of dominance in the light treatment's active community.

5. CONCLUSION

The combined activities of sunlight and microbes are responsible for the majority of carbon degradation in arctic freshwaters. However, little is known about the mechanisms of photochemical and biological DOM degradation or how they interact. To gain insight into these mechanisms and interactions, we manipulated DOM and microbial communities, and examined responses by coupling two state of the art technologies: high resolution mass spectrometry and metatranscriptomics.

Using FT-ICR MS, we determined that sunlight and microbes altered similar fractions of the DOM pool, including many identical DOM chemical formulas. These results suggested “competition” between photochemical and biological processes, and explained lower microbial activity in response to light-exposed DOM. FT-ICR MS results also suggested that photo- removal or photo-production of bioavailable compounds causes the contrasting effects of DOM photo-exposure on microbial activity, effects that have been documented many times, but remain unexplained.

Metatranscriptomics allowed further examination of the microbial response to light-exposed DOM, and indicated rapid reprogramming of community gene expression profiles. By identifying functional genes involved in this reprogramming, we revealed that shifts in microbial activity were associated with shifts in resource investment at the molecular level, providing another indication that photo-exposed DOM elicits shifts in microbial growth. Expression of certain functional genes also reflected changes in DOM

chemistry, providing new lines of evidence for sunlight's effect on DOM. This evidence was consistent with prior analytical studies, and suggested that sunlight degrades aromatics, oxidizes and decarboxylates DOM, and alters nutrient bioavailability.

Taken together, our findings indicate a complex interplay of photochemical and microbial DOM degradation. By paring FT-ICR MS and metatranscriptomics, we generated insight and new hypotheses about this interplay that could not have been achieved with other methods. Understanding the interactions of photochemical and biological DOM degradation is critical for predicting the fate of DOM in arctic surface waters, and ultimately the Arctic's role in climate change. As arctic soils thaw and DOM inputs to surface waters grow larger, interaction of photochemical and biological processes will determine the scales at which DOM is converted to CO_2. Here, we gained the kind of detailed perspective on these processes that is necessary to develop a predictive understanding of DOM degradation.

6. BIBLIOGRAPHY

1. Kling GW, Kipphut GW, Miller MC (1991) Arctic Lakes and Streams as Gas Conduits to the Atmosphere: Implications for Tundra Carbon Budgets. *Science 251*:298–301.

2. Rowland JC, et al. (2010) Arctic landscapes in transition: Responses to thawing permafrost. *Eos* 91:229–230.

3. Schuur EAG, et al. (2009) The effect of permafrost thaw on old carbon release and net carbon exchange from tundra. *Nature* 459:556–559.

4. Cole JJ, et al. (2007) Plumbing the global carbon cycle: Integrating inland waters into the terrestrial carbon budget. *Ecosystems* 10:171–184.

5. Cory RM, Ward CP, Crump BC, Kling GW (2014) Sunlight controls water column processing of carbon in arctic fresh waters. *Science* 345:925–928.

6. Obernosterer I, Reitner B, Herndl GJ (1999) Contrasting effects of solar radiation on dissolved organic matter and its bioavailability to marine bacterioplankton. *Limnol Oceanogr* 44:1645–1654.

7. Tranvik LJ, Bertilsson S (2001) Contrasting effects of solar UV radiation on dissolved organic sources for bacterial growth. *Ecol Lett* 4:458–463.

8. Vallieres C, Retamal L, Ramlal P, Osburn CL, Vincent WF (2008) Bacterial production and microbial food web structure in a large arctic river and the coastal Arctic Ocean. *J Mar Syst* 74:756–773.

9. Cory RM, Crump BC, Dobkowski J a, Kling GW (2013) Surface exposure to sunlight stimulates CO_2 release from permafrost soil carbon in the Arctic. *Proc Natl Acad Sci USA* 110:3429–34.

10. Crump BC, Kling GW, Bahr M, Hobbie JE (2003) Bacterioplankton Community Shifts in an Arctic Lake Correlate with Seasonal Changes in Organic Matter Source Bacterioplankton Community Shifts in an Arctic Lake Correlate with Seasonal Changes in Organic Matter Source. *Appl Environ Microbiol* 69:2253–2268.

11. Judd KE, Crump BC, Kling GW (2007) Bacterial responses in activity and community composition to photo-oxidation of dissolved organic matter from soil and surface waters. *Aquat Sci* 69:96–107.

12. Logue JB, et al. (2015) Experimental insights into the importance of aquatic bacterial community composition to the degradation of dissolved organic matter. *ISME J* 10:533-545.

13. Moran MA, Zepp RG (1997) Role of photoreactions in the formation of biologically labile compounds from dissolved organic matter. *Limnol Oceanogr* 42:1307–1316.

14. Mopper K, Kieber DJ, Stubbins A (2014) Marine Photochemistry of Organic Matter: Processes and Impacts. *Biogeochemistry of Marine Dissolved Organic Matter, Second Edition*: 389-450.

15. Hopkinson CS, et al. (1998) Terrestial imputs of organic matter to coastal ecosystems: An intercomparison of chemical characteristics and bioavailability. *Biogeochemistry* 43:221–234.

16. Cory RM, Kaplan LA (2012) Biological lability of streamwater fluorescent dissolved organic matter. *Limnol Oceanogr* 57:1347–1360.

17. Wetzel R (2003) Dissolved organic carbon: Detrital energetics, metabolic regulators, and drivers of ecosystem stability of aquatic ecosystems. *Aquatic Ecosystems- Interactivity of Dissolved Organic Matter*: 455-477.

18. Mann PJ, et al. (2012) Controls on the composition and lability of dissolved organic matter in Siberia's Kolyma River basin. *J Geophys Res Biogeosciences* 117:1–15.

19. Ward ND, et al. (2013) Degradation of terrestrially derived macromolecules in the Amazon River. *Nat Geosci* 6:530–533.

20. Frazier SW, Kaplan LA, Hatcher PG (2005) Molecular characterization of biodegradable dissolved organic matter using bioreactors and [$^{12}C/^{13}C$] tetramethylammonium hydroxide thermochemolysis GC-MS. *Environ Sci Technol* 39:1479–1491.

21. Volk CJ, Volk CB, Kaplan LA (1997) Chemical composition of biodegradable dissolved organic matter in streamwater. *Limnol Oceanogr* 42:39–44.

22. Sleighter RL, et al. (2014) A coupled geochemical and biogeochemical approach to characterize the bioreactivity of dissolved organic matter from a headwater stream. *J Geophys Res Biogeosciences* 119:1520–1537.

23. Frias-Lopez J, et al. (2011) Microbial community gene expression in ocean surface waters. *Proc Natl Acad Sci USA* 105:6–11.

24. McCarren J, et al. (2010) Microbial community transcriptomes reveal microbes and metabolic pathways associated with dissolved organic matter turnover in the sea. *Proc Natl Acad Sci USA* 107:16420–16427.

25. Poretsky RS, Sun S, Mou X, Moran MA (2010) Transporter genes expressed by coastal bacterioplankton in response to dissolved organic carbon. *Environ Microbiol* 12(3):616–627.

26. Ward CP, Cory RM (2015) Chemical composition of dissolved organic matter draining permafrost soils. *Geochim Cosmochim Acta* 167:63–79.

27. Ward CP, Cory RM (2016) Complete and partial photo-oxidation of dissolved organic matter draining permafrost soils. *Environ Sci Technol* 50:3545-3553

28. Kling GW, Kipphut GW, Miller MM, O'Brien WJ (2000) Integration of lakes and streams in a landscape perspective: The importance of material processing on spatial patterns and temporal coherence. *Freshw Biol* 43:477–497.

29. Crump BC, Baross JA, Simenstad CA (1998) Dominance of particle-attached bacteria in the Columbia River estuary, USA. *Aquat Microb Ecol* 14:7–18.

30. Poretsky RS, et al. (2009) Comparative day/night metatranscriptomic analysis of microbial communities in the North Pacific subtropical gyre. *Environ Microbiol* 11:1358–1375.f

31. Zhou J, Bruns MA, Tiedje JM (1996) DNA recovery from soils of diverse composition. *Appl Environ Microbiol* 62:316–322.

32. Helms JR, et al. (2008) Absorption spectral slopes and slope ratios as indicators of molecular weight, source, and photobleaching of chromophoric dissolved organic matter. *Limonology Oceanogr* 53:955–969.

33. Remucal CK, Cory RM, Sander M, McNeill K (2012) Low molecular weight components in an aquatic humic substance as characterized by membrane dialysis and Orbitrap mass spectrometry. *Environ Sci Technol* 46:9350–9359.

34. R Core Team (2013) R: A language and environment for statistical

computing. R Foundation for Statistical Computing, Vienna, Austria. http://www.R-project.org/.

35. Bushnell B (2015) BBMap. http://sourceforge.net/projects/bbmap

36. Li D, Liu CM, Luo R, Sadakane K, Lam TW (2015) MEGAHIT: An ultra-fast single-node solution for large and complex metagenomics assembly via succinct de Bruijn graph. *Bioinformatics* 31:1674–1676.

37. Hyatt D, et al. (2010) Prodigal: prokaryotic gene recognition and translation initiation site identification. *BMC Bioinformatics* 11:119.

38. Kanehisa M, Goto S (2000) KEGG: Kyoto Encyclopaedia of Genes and Genomes. *Nucl Acids Res* 28:27–30.

39. Huntemann M, et al. (2015) The Standard Operating Procedure of the DOE-JGI Microbial Genome Annotation Pipeline (MGAP v. 4) Keywords. *Stand Genomic Sci* 10:86.

40. Langmead B, Salzberg SL (2012) Fast gapped-read alignment with Bowtie 2. *Nat Methods* 9:357–359.

41. Li H, et al. (2009) The Sequence Alignment/Map format and SAMtools. *Bioinformatics* 25:2078–2079.

42. Wagner GP, Kin K, Lynch VJ (2012) Measurement of mRNA abundance using RNA-seq data: RPKM measure is inconsistent among samples. *Theory Biosci* 131:281–285.

43. Legendre P & Legendre L (1998) Numerical Ecology. Elsevier Science B.V., Amsterdam.

44. Oksanen J (2007) Multivariate analyses of ecological communities in R: vegan tutorial. 39pp, http://cc.oulu.fi/jarioksa/opetus/metodi/vegantutor.pdf

45. Wickham, H (2009) ggplot2: Elegant Graphics for Data Analysis. Springer-Verlag, New York.

46. Murdoch DJ & Chow ED (1996). A graphic display of large correlation matrices. *The American Statistician* 50: 178-180.

47. Huson DH, Richter DC, Mitra S, Auch AF, Schuster SC (2009) Methods for comparative metagenomics. *BMC Bioinformatics* 10 Suppl 1:S12.

48. Nayfach S, et al. (2015) Automated and Accurate Estimation of Gene Family Abundance from Shotgun Metagenomes. *PLoS Comput Biol* 11:1–29.

49. Schloss PD, et al. (2009) Introducing mothur: Open-source, platform-independent, community-supported software for describing and comparing microbial communities. *Appl Environ Microbiol* 75:7537–7541.

50. Caporaso JG, et al. (2010) QIIME allows analysis of high- throughput community sequencing data. *Nat Publ Gr* 7:335–336.

51. Koehler B, Landelius T, Weyhenmeyer GA, Machida N, Tranvik LJ (2014) Sunlight-induced carbon dioxide emissions from inland waters. *Glob Biogeochem Cylces* 28:696–711.

52. Strome D, Miller M (1978) Photolytic changes in dissolved humic substances. *Verh Internat Verein Limnol* 29:1248–1254.

53. Wetzel RG, Hatcher PG, Bianchi TS (1995) Natural photolysis by ultraviolet irradiance of recalcitrant dissolved organic matter to simple substrates for rapid bacterial metabolism. *Limnol Oceanogr* 40:1369–1380.

54. Moran MA, Sheldon WM, Zepp RG (2000) Carbon loss and optical property changes during long-term photochemical and biological degradation of estuarine dissolved organic matter. *Limnol Oceanogr* 45:1254–1264.

55. Hudson N, Baker A, Reynolds D (2007) Fluorescence Analysis of DOM in Natural, Waste & Polluted Waters-- A Review. *River Res Appl* 23:631–649.

56. Gonsior M, et al. (2009) Photochemically Induced Changes in Dissolved Organic Matter Identified by Ultrahigh Resolution Fourier Transform Ion Cyclotron Resonance Mass Spectrometry. *Environ Sci Technol* 43:698–703.

57. Stubbins A, et al. (2010) Illuminated darkness: Molecular signatures of Congo River dissolved organic matter and its photochemical alteration as revealed by ultrahigh precision mass spectrometry. *Limnol Oceanogr* 55:1467–1477.

58. Gonsior M, Schmitt-Kopplin P, Bastviken D (2013) Depth-dependent molecular composition and photo-reactivity of dissolved organic matter in a boreal lake under winter and summer conditions. *Biogeosciences*

10:6945–6956.

59. Gonsior M, et al. (2014) Photochemical production of polyols arising from significant photo-transformation of dissolved organic matter in the oligotrophic surface ocean. *Mar Chem* 163:10–18.

60. D'Andrilli J, Cooper WT, Foreman CM, Marshall AG (2015) An ultrahigh-resolution mass spectrometry index to estimate natural organic matter lability. *Rapid Commun Mass Spectrom* 29:2385–2401.

61. Miles CJ, Brezonik PL (1981) Oxygen consumption in humic-colored waters by a photochemical ferrous-ferric catalytic cycle. *Environ Sci Technol* 15:1089–1095.

62. Fuchs G, Boll M, Heider J (2011) Microbial degradation of aromatic compounds — from one strategy to four. *Nat Rev Microbiol* 9:803–816.

63. Iwai S, et al. (2010) Gene-targeted-metagenomics reveals extensive diversity of aromatic dioxygenase genes in the environment. *ISME J* 4:279–285.

64. Benner R, Biddanda B (1998) Photochemical transformations of surface and deep marine dissolved organic matter : Effects on bacterial growth. 43:1373–1378.

65. Abboudi M, et al. (2008) Effects of photochemical transformations of dissolved organic matter on bacterial metabolism and diversity in three contrasting coastal sites in the Northwestern Mediterranean Sea during summer. *Microb Ecol* 55:344–357.

66. Amado AM, Cotner JB, Cory RM, Edhlund BL, McNeill K (2014) Disentangling the Interactions Between Photochemical and Bacterial Degradation of Dissolved Organic Matter: Amino Acids Play a Central Role. *Microb Ecol* 69:554-566.

67. de Menezes A, Clipson N, Doyle E (2012) Comparative metatranscriptomics reveals widespread community responses during phenanthrene degradation in soil. *Environ Microbiol* 14:2577–2588.

68. Shi Y, McCarren J, Delong EF (2012) Transcriptional responses of surface water marine microbial assemblages to deep-sea water amendment. *Environ Microbiol* 14:191–206.

69. Teeling H, et al. (2012) Substrate-Controlled Succession of Marine Bacterioplankton Populations Induced by Phytoplankton Bloom. *Science* 336:608–611.

70. Nomura M, Gourse R, Baughman G (1984) Regulation of the Synthesis of Ribosomes and Ribosomal Components. *Ann Rev Biochem* 53:75–117.

71. Kraakman LS, et al. (1993) Growth-related expression of ribosomal protein genes in Saccharomyces cerevisiae. *Mol Gen Genet* 239:196–204.

72. Rolfe MD, et al. (2011) Lag phase is a distinct growth phase that prepares bacteria for exponential growth and involves transient metal accumulation. *J Bacteriol* 194:686–701.

73. Madar D, et al. (2013) Promoter activity dynamics in the lag phase of Escherichia coli. *BMC Syst Biol* 7:136.

74. Scott M, Mateescu EM, Zhang Z, Hwa T (2010) Interdependence of Cell Growth Origins and Consequences. *Science* 330:1099–1102.

75. Chang DE, Smalley DJ, Conway T (2002) Gene expression profiling of Escherichia coli growth transitions: An expanded stringent response model. *Mol Microbiol* 45:289–306.

76. Clark ME, et al. (2006) Temporal transcriptomic analysis as Desulfovibrio vulgaris Hildenborough transitions into stationary phase during electron donor depletion. *Appl Environ Microbiol* 72:5578–5588.

77. Pérez M-T, Sommaruga R (2006) Differential effect of algal- and soil-derived dissolved organic matter on alpine lake bacterial community composition and activity. *Limnol Oceanogr* 51:2527–2537.

78. Soutourina OA, Bertin PN (2003) Regulation cascade of flagellar expression in Gram-negative bacteria. *FEMS Microbiol Rev* 27:505–523.

79. Monod J (1949) The Growth of Bacterial Cultures. *Annu Rev M* 3:371–394.

80. Schultz D, Kishony R (2013) Optimization and control in bacterial Lag phase. *BMC Biol* 11:120.

81. Wershaw RL (1989) Application of a membrane model to the sorptive interactions of humic substances. *Environ Health Perspect* 83:191–203.

82. Shiller AM, Duan S, van Erp P, Bianchi TS (2006) Photo-oxidation of

dissolved organic matter in river water and its effect on trace element speciation. *Limnol Oceanogr* 51:1716–1728.

83. Bushaw KL, et al. (1996) Photochemical release of biologically available nitrogen from aquatic dissolved organic matter. *Nature* 381:404–407.

84. Francko DA, Heath RT (1982) UV-sensitive complex phosphorus: association with dissolved humic material and iron in a bog lake. *Limnol Ocean* 27:564–569.

85. Vähätalo A V., Salonen K, Münster U, Järvinen M, Wetzel RG (2003) Photochemical transformation of allochthonous organic matter provides bioavailable nutrients in a humic lake. *Arch fur Hydrobiol* 156:287–314.

86. Hewson I, Poretsky RS, Tripp HJ, Montoya JP, Zehr JP (2010) Spatial patterns and light-driven variation of microbial population gene expression in surface waters of the oligotrophic open ocean. *Environ Microbiol* 12:1940–1956.

87. Scheck CK, Frimmel FH (1995) Degradation of phenol and salicylic acid by ultraviolet radiation/hydrogen peroxide/oxygen. *Water Res* 29:2346–2352.

88. Opsahl S, Benner R (1998) Photochemical reactivity of dissolved lignin in river and ocean waters. *Limnol Oceanogr* 43:1297–1304.

89. Bugg TDH, Ahmad M, Hardiman EM, Singh R (2011) The emerging role for bacteria in lignin degradation and bio-product formation. *Curr Opin Biotechnol* 22:394–400.

90. Gulvik C a, Buchan A (2013) Simultaneous catabolism of plant-derived aromatic compounds results in enhanced growth for members of the Roseobacter lineage. *Appl Environ Microbiol* 79:3716–23.

91. Cory RM, et al. (2010) Singlet oxygen in the coupled photochemical and biochemical oxidation of dissolved organic matter. *Environ Sci Technol* 44:3683–3689.

92. Page SE, Logan JR, Cory RM, McNeill K (2014) Evidence for dissolved organic matter as the primary source and sink of photochemically produced hydroxyl radical in arctic surface waters. *Environ Sci Process Impacts* 16:807–22.

93. Kujawinski EB, Del Vecchio R, Blough N V., Klein GC, Marshall AG

(2004) Probing molecular-level transformations of dissolved organic matter: Insights on photochemical degradation and protozoan modification of DOM from electrospray ionization Fourier transform ion cyclotron resonance mass spectrometry. *Mar Chem* 92:23–37.

94. Schmitt-Kopplin P, Hertkorn N, Schulten H-R, Kettrup A (1998) Structural Changes in a Dissolved Soil Humic Acid during Photochemical Degradation Processes under O_2 and N_2 Atmosphere. *Environ Sci Technol* 32:2531–2541.

95. Anesio AM, Granéli W, Aiken GR, Kieber DJ, Mopper K (2005) Effect of humic substance photodegradation on bacterial growth and respiration in lake water. *Appl Environ Microbiol* 71:6267–6275.

96. Xie H, Zafiriou OC, Cai WJ, Zepp RG, Wang Y (2004) Photooxidation and its effects on the carboxyl content of dissolved organic matter in two coastal rivers in the southeastern United States. *Environ Sci Technol* 38:4113–4119.

97. Ishige T, Krause M, Bott M, Wendisch VF, Sahm H (2003) The Phosphate Starvation Stimulon of *Corynebacterium glutamicum* Determined by DNA Microarray Analyses. *J Bacteriol* 185:4519–4529.

98. Cotner JBJ, Heath RT (1990) Iron redox effects on photosensitive phosphorus release from dissolved humic materials. *Limnol Oceanogr* 35:1175–1181.

99. Zhang Y, et al. (2013) Photobleaching Response of Different Sources of Chromophoric Dissolved Organic Matter Exposed to Natural Solar Radiation Using Absorption and Excitation-Emission Matrix Spectra. *PLoS One* 8: e77515.

100. Gobler C, Hutchins D, Nicholas S, Cosper E, Sanudo-Wilhelmy S (1997) Release and bioavailability of C, N, P, Se, and Fe following viral lysis of a chrysophyte. *Limnol Oceanogr* 42:1492–1504.

101. Jorgensen NOG, Tranvik L, Edling H, Graneli W, Lindell M (1998) Effects of sunlight on occurrence and bacterial turnover of specific carbon and nitrogen compounds in lake water. *FEMS Microbiol Ecol* 25:217–227.

102. McCallister SL, Bauer JE, Kelly J, Ducklow HW (2005) Effects of sunlight on decomposition of estuarine dissolved organic C, N and P and bacterial metabolism. *Aquat Microb Ecol* 40:25–35.

103. Wiegner TN, Seitzinger SP (2001) Photochemical and microbial

degradation of external dissolved organic matter inputs to rivers. *Aquat Microb Ecol* 24:27–40.

104. Francko, DA (1990) Alteration of bioavailability and toxicity by phototransformation of organic acids. *Organic Acids in Aquatic Systems.* John Wiley & Sons, New York, NY, 167–177.

105. Cronan JE, Rock CO (2008) Biosynthesis of Membrane Lipids. *EcoSal Plus* 3.1.

106. Ames GF (1986) Bacterial Periplasmic Transport Systems: Structure, Mechanism, and Evolution. *Ann Rev Biochem* 55:397-425.

107. Merchant SS, Helmann JD (2012) Elemental Economy: Microbial Strategies for Optimizing Growth in the Face of Nutrient Limitation. *Adv Microb Physiol* 60: 91–210.

108. Bushaw-Newton KL, Moran MA (1999) Photochemical formation of biologically available nitrogen from dissolved humic substances in coastal marine systems. *Aquat Microb Ecol* 18:285–292.

109. Amador JA, Alexander M, Zika RG (1989) Sequential Photochemical and Microbial Degradation of Organic Molecules Bound to Humic Acid Sequential Photochemical and Microbial Degradation of Organic Molecules Bound to Humic Acid. *Appl Environ Microbiol* 55:2843–2849.

110. Sekowska A, Kung H (2000) Sulfur metabolism in *Escherichia coli* and Related Bacteria: Facts and Fiction. *J Mol Microbiol Biotechnol* 2:145-177.

111. Sandy M, Butler A (2009) Microbial iron acquisition: Marine and terrestrial siderophores. *Chem Rev* 109:4580–4595.

112. Voelker BM, Morel FMM, Sulzberger B (1997) Iron redox cycling in surface waters: Effects of humic substances and light. *Environ Sci Technol* 31:1004–1011.

113. Janssen PH (2006) Identifying the Dominant Soil Bacterial Taxa in Libraries of 16S rRNA and 16S rRNA Genes. *Appl Environ Microbiol* 72:1719–1728.

114. Crump BC, Amaral-Zettler LA, Kling GW (2012) Microbial diversity in arctic freshwaters is structured by inoculation of microbes from soils. *ISME J* 6:1629–1639.

115. Massana R, Pedros-Alio C, Casamayor EO, Gasol JM (2001) Changes in marine bacterioplankton phylogenetic composition during incubations designed to measure biogeochemically significant parameters. *Limnol Oceanogr* 46:1181–1188.

116. Fuchs BM, Zubkov M V., Sahm K, Burkill PH, Amann R (2000) Changes in community composition during dilution cultures of marine bacterioplankton as assessed by flow cytometric and molecular biological techniques. *Environ Microbiol* 2:191–201.

117. Bouvier T, Del Giorgio PA (2007) Key role of selective viral-induced mortality in determining marine bacterial community composition. *Environ Microbiol* 9:287–297.

118. Moran MA, et al. (2007) Ecological genomics of marine roseobacters. *Appl Environ Microbiol* 73:4559–4569.

119. Widada J, et al. (2002) Molecular detection and diversity of polycyclic aromatic hydrocarbon-degrading bacteria isolated from geographically diverse sites. *Appl Microbiol Biotechnol* 58:202–209.

120. Zocca C, Di Gregorio S, Visentini F, Vallini G (2004) Biodiversity amongst cultivable polycyclic aromatic hydrocarbon- transforming bacteria isolated from an abandoned industrial site. *FEMS Microbiol Lett* 238:375–382.

121. Wu Y, et al. (2008) Bioremediation of polycyclic aromatic hydrocarbons contaminated soil with *Monilinia* sp.: Degradation and microbial community analysis. *Biodegradation* 19:247–257.

122. Baldrian P, et al. (2012) Active and total microbial communities in forest soil are largely different and highly stratified during decomposition. *ISME J* 6:248–258.

123. Kolter R, Siegele DA, Tormo A (1993) The stationary phase of the bacterial life cycle. *Annu Rev Microbiol* 47:855–874.

124. Jones SE, Lennon JT (2010) Dormancy contributes to the maintenance of microbial diversity. *Proc Natl Acad Sci USA* 107:5881–6.

125. Sangwan P, Kovac S, Davis KER, Sait M, Janssen PH (2005) Detection and cultivation of soil Verrucomicrobia. *Appl Environ Microbiol* 71:8402–8410.

126. Thomas F, Hehemann JH, Rebuffet E, Czjzek M, Michel G (2011)

Environmental and gut Bacteroidetes: The food connection. *Front Microbiol* 2:1–16.

127. Edwards JL, et al. (2010) Identification of carbohydrate metabolism genes in the metagenome of a marine biofilm community shown to be dominated by Gammaproteobacteria and Bacteroidetes. *Genes* 1:371–384.

128. Gómez-Pereira PR, et al. (2012) Genomic content of uncultured Bacteroidetes from contrasting oceanic provinces in the North Atlantic Ocean. *Environ Microbiol* 14:52–66.

7. FIGURES

Figure 1. Schematic of experimental design.

Figure 2. Effect of photochemical and biological degradation on DOM.

Figure 3. Microbial activity across treatments.

Figure 4. Characterization of gene expression across treatments.

Figure 5. Expression of KEGG tier II and III categories across treatments.

Figure 6. Genetic evidence for sunlight's effect on DOM.

Figure 7. Taxonomic composition of whole and active communities.

Figure 1. Schematic of experimental design.

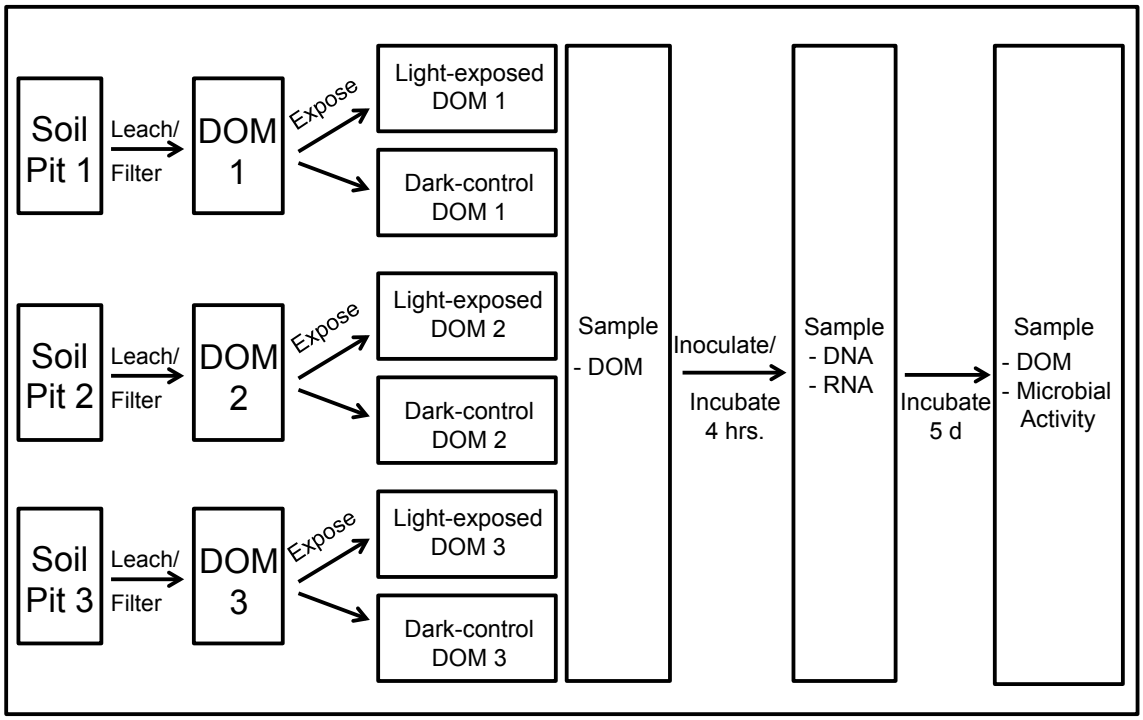

Figure 2. Effect of photochemical and biological degradation on DOM. The van Krevelen diagram shows FT-ICR MS formulas that were produced by sunlight (gray), degraded by sunlight (blue), and degraded by bacteria (red).

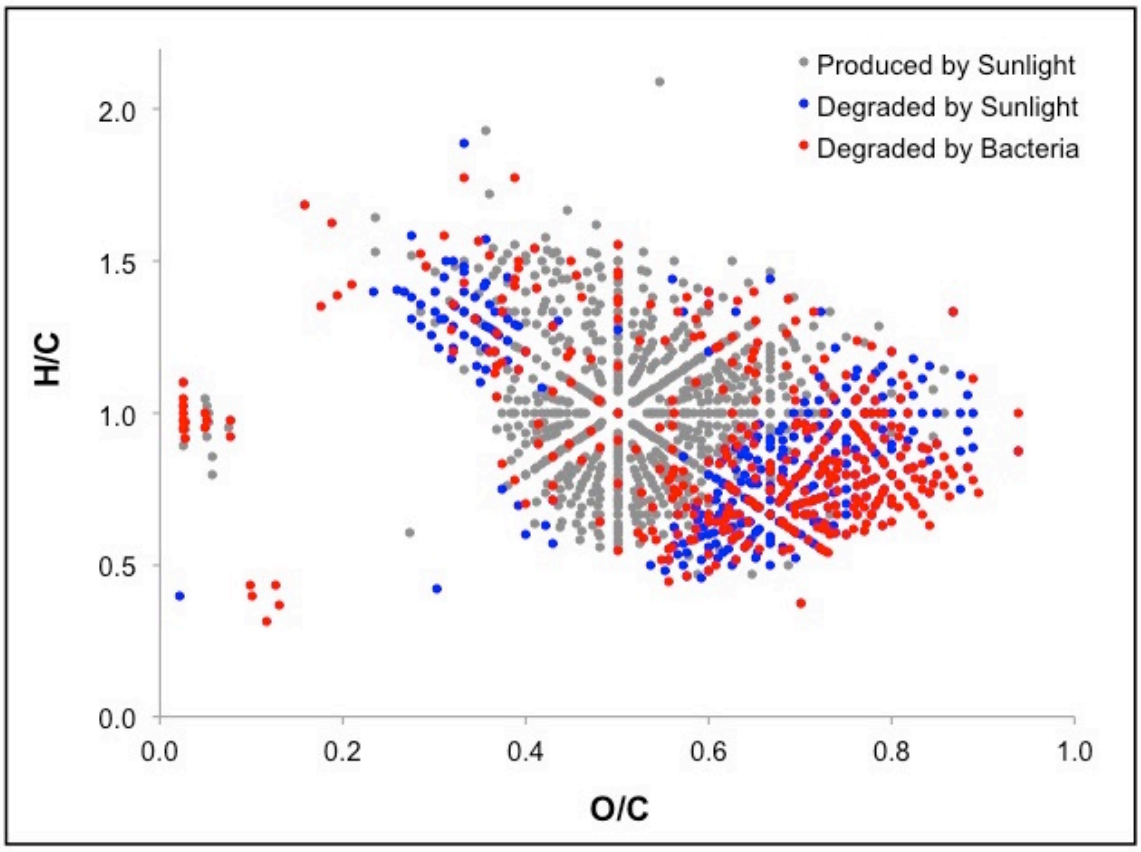

Figure 3. Microbial activity in light-exposed (light gray) and dark-control (dark gray) treatments, as measured by respiration (O_2 consumption and CO_2 production), biomass production, new cell production, and growth efficiency.

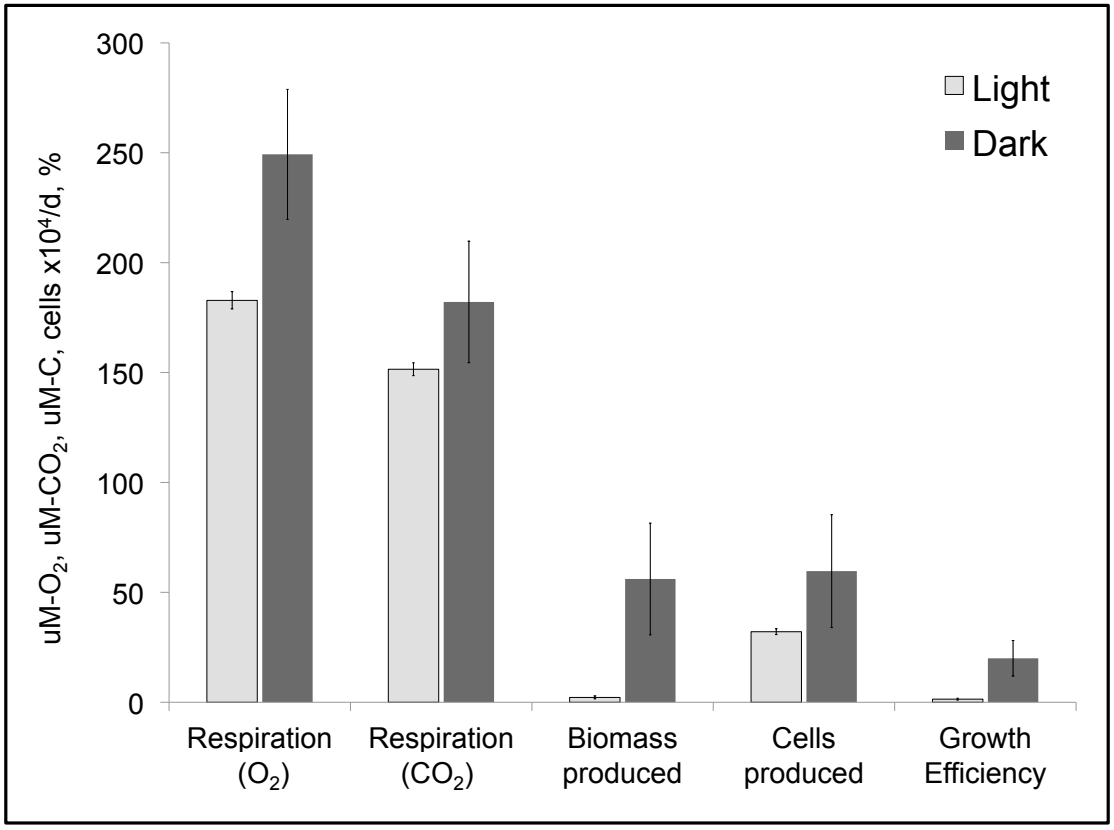

Figure 4. Characterization of gene expression across treatments.
(a) Nonmetric multidimensional scaling analysis of metatranscriptomes from light-exposed (light gray) and dark-control (dark gray) treatments. Ellipses represent 95% confidence intervals, as measured by standard error. (b) Shannon alpha diversity each treatment. (c) Scatterplot representing mean transcript abundance of all genes (KOs) in the light-exposed versus dark-control treatments (gray), and of select genes (green) that cumulatively contributed to the top 30% of dissimilarity between treatments according to SIMPER. The 1:1 line (black) highlights differences in transcript abundance of many genes across treatments. Points plotted on the axes are genes with zero measured abundance in one treatment but not the other.

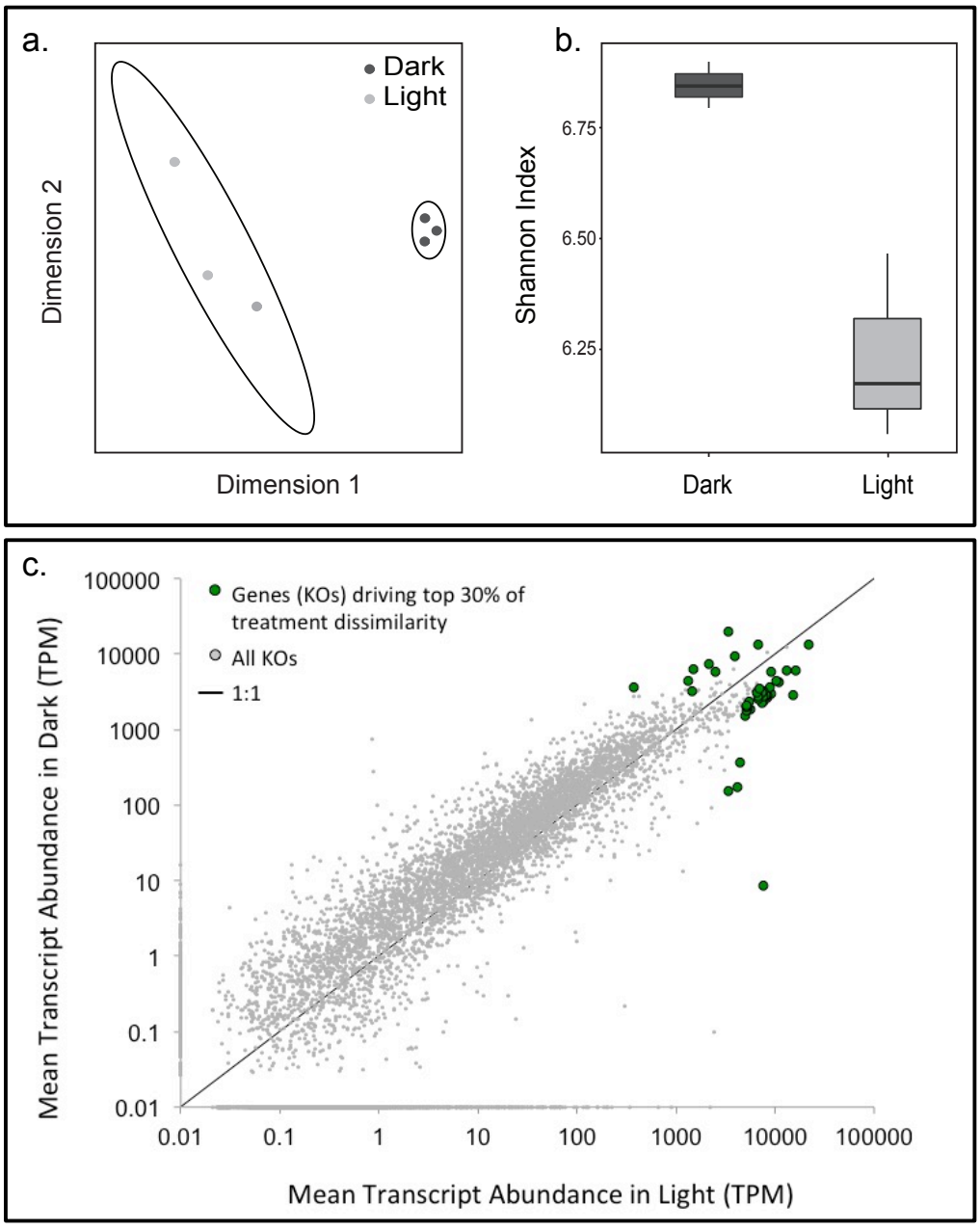

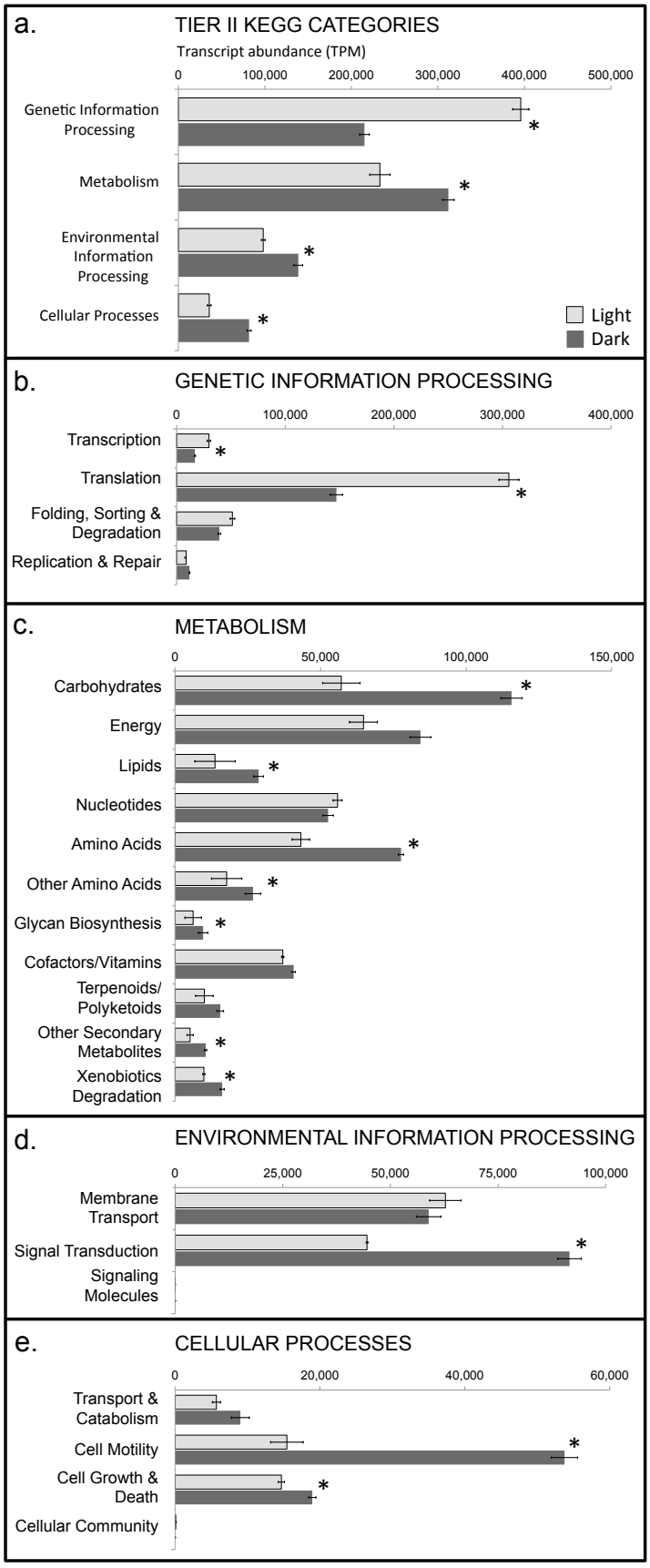

Figure 5. Expression of KEGG tier II (a) and III (b-e) categories in light-exposed (light gray) and dark-control (dark gray) treatments. Asterisks represent significant differences according to

Figure 6. Genetic evidence for sunlight's effect on DOM. Heat-maps represent transcript abundance of specific categories of enzyme and transporter genes for each replicate. Dark red represents the lowest values and light yellow represents the highest values. (a) All differentially expressed genes (paired t-test, $p \leq 0.05$) in aromatic degradation, oxygenase, and decarboxylase categories. (b) All differentially expressed genes in phosphorus, amino acid, sugar, polyol, and inorganic ion ABC transporter categories (paired t-test, $p \leq 0.05$). One asterisk (*) indicates aromatic degradation genes that are duplicated because they also fall into the decarboxylase or oxygenase category, and two asterisks (**) indicates a non-significant difference between treatments ($p = 0.17$) for the iron(III) transporter.

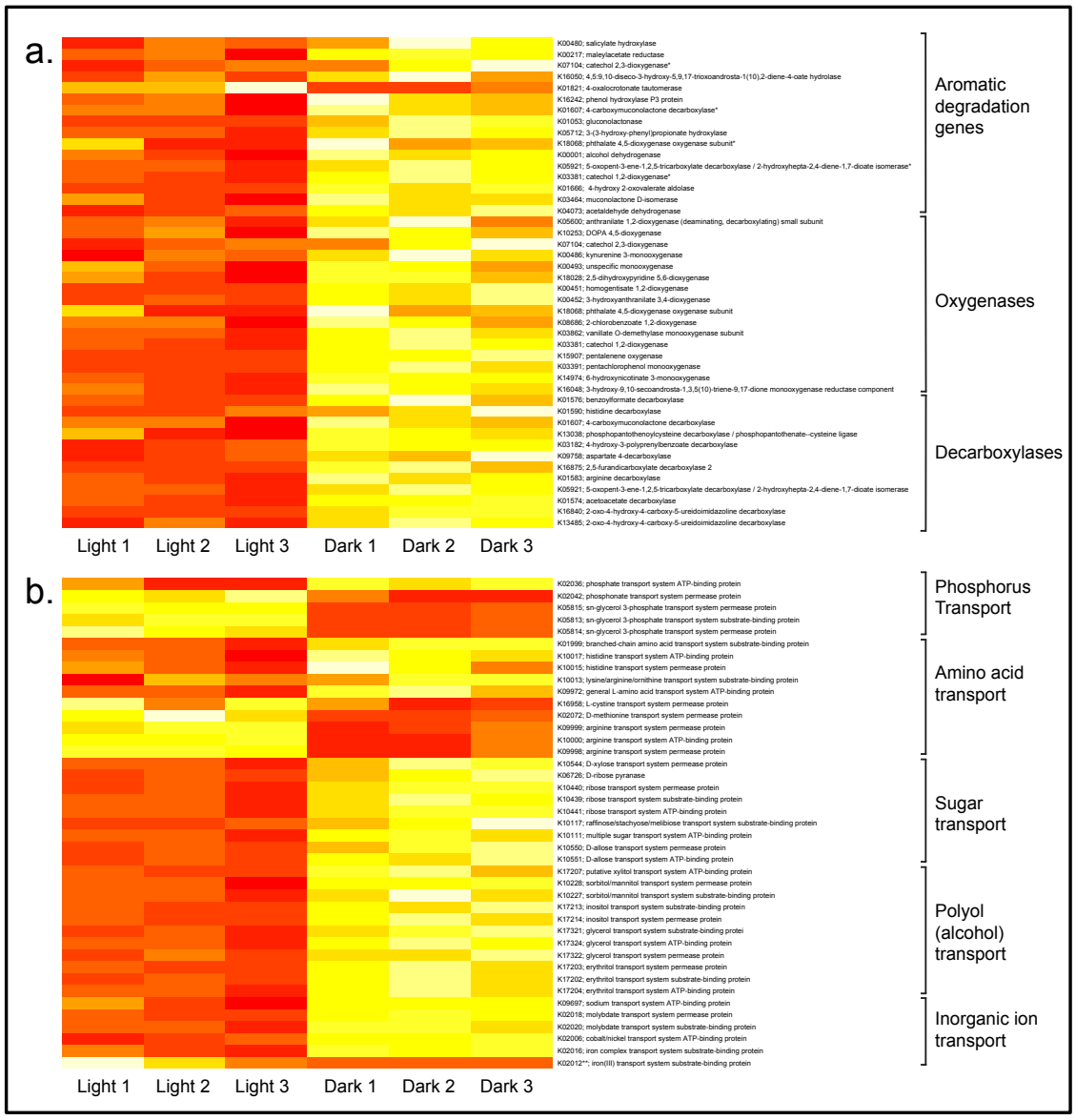

Figure 7. Relative taxonomic composition of the whole community (16S amplicons), the active community (metatranscriptomes), and communities expressing genes in KEGG pathways for Ribosome, DNA Replication, TCA Cycle, and Degradation of Aromatic Compounds.